

Palaeoenvironmental and palaeoecological reconstructions based on oxygen, carbon and sulfur isotopes of Early Permian shark spines from the French Massif central

Vincent Luccisano, Gilles Cuny, Alan Pradel, François Fourel, Christophe Lécuyer, Jean-Marc Pouillon, Kathleen Lachat, Romain Amiot

▶ To cite this version:

Vincent Luccisano, Gilles Cuny, Alan Pradel, François Fourel, Christophe Lécuyer, et al.. Palaeoenvironmental and palaeoecological reconstructions based on oxygen, carbon and sulfur isotopes of Early Permian shark spines from the French Massif central. Palaeogeography, Palaeoclimatology, Palaeoecology, 2023, 628, pp.111760. 10.1016/j.palaeo.2023.111760. hal-04554856

HAL Id: hal-04554856 https://hal.science/hal-04554856

Submitted on 22 Apr 2024

HAL is a multi-disciplinary open access archive for the deposit and dissemination of scientific research documents, whether they are published or not. The documents may come from teaching and research institutions in France or abroad, or from public or private research centers. L'archive ouverte pluridisciplinaire **HAL**, est destinée au dépôt et à la diffusion de documents scientifiques de niveau recherche, publiés ou non, émanant des établissements d'enseignement et de recherche français ou étrangers, des laboratoires publics ou privés.

1	Palaeoenvironmental and palaeoecological reconstructions based on oxygen, carbon and
2	sulfur isotopes of Early Permian shark spines from the French Massif central
3	Vincent Luccisano ^{1,2*} , Gilles Cuny ² , Alan Pradel ³ , François Fourel ² , Christophe Lécuyer ¹ ,
4	Jean-Marc Pouillon ⁴ , Kathleen Lachat ¹ , Romain Amiot ¹
5	
6	¹ Univ Lyon, UCBL, ENSL, UJM, CNRS, LGL-TPE, F-69622, Villeurbanne, France;
7	² Univ Lyon, Université Claude Bernard Lyon 1, CNRS, ENTPE, UMR 5023 LEHNA, F-
8	69622, Villeurbanne, France;
9	³ CR2P - Centre de Recherche en paléontologie - Paris ; Muséum National d'Histoire
10	Naturelle - Centre National de la Recherche Scientifique- Sorbonne Université. France;
11	⁴ Rhinopolis Association, 179 rue des Plattières 38300 Nivolas Vermelle/BP 39 03800 Gannat,
12	France.
13	
14	RH: Isotopic compositions of French Permian aquatic faunas
15	
16	*Corresponding author. Email: vincent.luccisano@gmail.com
17	
18	
19	
20	
21	
22	
23	
24	

25 Abstract

The palaeoecology of the Xenacanthiformes (Chondrichthyes) is still a matter of 26 discussion. Historically considered as freshwater organisms, hypotheses of euryhaline ecology 27 including migratory behaviour were recently proposed based on the histology of their dorsal 28 spines. However, recent studies still argued for a full freshwater ecology based on the 29 geochemical compositions of their teeth. Their ecology is particularly interesting to 30 31 investigate for those coming from the environmentally ambiguous Early Permian intra-32 mountainous localities of Buxières-les-Mines (Bourbon-l'Archambault Basin, Allier) and the Muse oil-shale bed (OSB) (Autun Basin, Saône-et-Loire) from the French Massif central. 33 34 These two localities were interpreted as freshwater settings but doubts on marine influences 35 exist. To assess their palaeoenvironment and the palaeoecology settings based on xenacanthiforms occurrences, we have analysed the stable isotope compositions ($\delta^{18}O$, $\delta^{13}C$ 36 and δ^{34} S) of the bioapatite of their vertebrate faunas. From these stable isotope compositions, 37 we interpret that Buxières-les-Mines was a large and deep freshwater lake, equivalent to the 38 39 modern Indonesian Lake Matano, whereas the Muse OSB is interpreted as a shallow tropical 40 lake with drying up events, equivalent to the Lake Punta Laguna, Amazonia or the Lake Tanganyika, Africa. The oxygen isotope compositions of the xenacanth dorsal spines of 41 42 Buxières-les-Mines are relatively constant from the apex to the base. Such uniform isotopic compositions recorded during the life of xenacanths support either their sedentary lifestyle or 43 stenohalinity. The apparent ability of small xenacanthiforms to endure drying up, as shown by 44 the variations in isotope composition of the Muse OSB specimens, could explain their 45 resilience during the Early Permian whereas Carboniferous xenacanthiforms occurring in 46 47 large lake and river systems almost disappeared.

48

Keywords: Stable isotope; geochemistry; Xenacanthiformes; late Palaeozoic; dorsal spine

51 **1. Introduction**

Xenacanthiformes is an order of Palaeozoic chondrichthyans characterised by an eellike body, diplodont teeth and an ever-growing dorsal spine (e.g. Zangerl 1981; Ginter et al.,
2010). It is divided into two families (e.g. Ginter et al., 2010): the Diplodoselachidae that
exhibit a rounded dorsal spine with two posterior rows of denticles whereas the
Xenacanthidae have a dorso-ventrally compressed dorsal spine which bears two lateral rows
of denticles.

Most of the time, they have been recovered from ancient lacustrine or palustrine 58 deposits (Zangerl, 1981; Compagno, 1990; Kriwet et al., 2008). Consequently, some authors 59 (e.g. Schneider et al., 2000; Fischer et al., 2013, 2014; Štamberg et al., 2016) have interpreted 60 them as a proxy of freshwater environments. However, numerous studies (Schultze, 1985, 61 62 1995, 1998, 2009, 2013; Olson, 1989; Soler-Gijón, 1993; Johnson, 1999; Soler-Gijón and Moratalla, 2001; Schultze and Soler-Gijón, 2004; Hampe et al., 2006; Laurin and Soler-Gijón, 63 2010; Carpenter et al., 2011; Beck et al., 2016) questioned their full freshwater-adaptation and 64 65 argued in favour of a possible euryhaline ecology.

66 To test the different hypotheses concerning their environmental adaptations, recent studies have investigated the phosphate oxygen isotope composition ($\delta^{18}O_p$) of teeth from 67 68 some Carboniferous and Permian xenacanthiforms from North America and Europe (Fischer et al., 2013, 2014). Xenacanthiforms were thus interpreted as full freshwater organisms living 69 in environments experiencing significant drying events. However, other recent studies (e.g. 70 Soler-Gijón and Moratalla, 2001; Schultze and Soler-Gijón, 2004; Hampe et al., 2006; 71 Schultze, 2009; Laurin and Soler-Gijón, 2010; Carpenter et al., 2011) advocated for an 72 euryhaline behaviour. These interpretations were supported by conclusions of Soler-Gijón 73 (1999) and Beck et al., (2016) who focused on the histological structure of the dorsal spine of 74 American and European Orthacanthus and who argued for an euryhaline ecology with 75

diadromous and catadromous migrations. These conflicting interpretations of xenacanthiforms
palaeoecology emphasise the need to provide new investigations on this topic.

This is particularly true for xenacanthiforms from environmentally ambiguous basins 78 like that of Bourbon-l'Archambault (Allier, France) in the French Massif central. Fischer et 79 al. (2013) interpreted the $\delta^{18}O_p$ of teeth and dorsal spines of *Orthacanthus buxieri* from the 80 Buxières-les-Mines locality in agreement with a freshwater living environment. However, 81 82 Schultze and Soler-Gijón (2004) and Schultze (2009) listed faunal components of nearby localities from the French Massif central that could indicate a probable marine influence. In 83 addition, the palaeoenvironment of the nearby Muse oil-shale bed (OSB) locality in the Autun 84 85 Basin (Saône-et-Loire, France) has been widely investigated by Mercuzot (2020) and Mercuzot et al. (2022) from a sedimentological point of view. Doubts persist for this locality, 86 which has also provided xenacanthiform remains. Depending on the used methods, the Muse 87 88 OSB can be considered as a distal or coastal freshwater lake, but none of these hypotheses have been tested by geochemical analyses on xenacanthiform hard tissues up to now. 89 In this work, we test the hypothesis of a strict freshwater palaeoecology of the 90 Xenacanthiformes from Buxières-les-Mines and the Muse OSB. We investigate the phosphate 91 oxygen ($\delta^{18}O_p$), carbonate oxygen and carbon ($\delta^{18}O_c$ and $\delta^{13}C_c$) and the sulfur isotope 92 compositions (δ^{34} S) of the bioapatite along their dorsal spines in order to define 1) their living 93 environment and 2) its potential changes during their lifetime. To better constrain the 94 environmental reconstruction, we also investigated the whole associated aquatic vertebrate 95 96 faunas composed of acanthodian fin spines, actinopterygian ganoid scales and temnospondyl bones. 97

98

99 2. Geological context

The Bourbon-l'Archambault Basin is located in the Northern Massif central (Fig. 1C; 100 101 Allier, France; Châteauneuf 1980; Châteauneuf and Farjanel 1989) and is part of a large set of Carboniferous-Permian non-marine basins (Fig. 1A; Gand et al., 2015, 2017). It is structurally 102 divided into two sub-basins (Châteauneuf and Farjanel, 1989; Stever et al., 2000): the 103 Aumance sub-basin in the West and the Souvigny sub-basin in the East. The sedimentary 104 deposits, which are mostly composed of conglomerates, alluvial arkoses, palustrine coal 105 106 seams, bituminous black shales, fluvial sandstones and thin pyroclastic horizons (Roscher and Schneider, 2006), extend stratigraphically from the Late Carboniferous to the Triassic (e.g. 107 Steyer et al., 2000). For some authors (Roscher and Schneider, 2006; Steyer et al., 2000), this 108 109 basin is characteristic of a freshwater environment, even if some doubts remain about 110 potential marine influences (Schultze and Soler-Gijón, 2004; Schultze, 2009).

The former open-cast coal mine of Buxières-les-Mines is a fossiliferous locality 111 located in the southern part of the Aumance sub-basin (Fig. 1C; Steyer et al., 2000). 112 Stratigraphically (Fig. 1E), Buxières-les-Mines is situated in the Supra-Buxières Member in 113 the upper part of the Buxières Formation (Steyer et al., 2000). Even if the Carboniferous-114 Permian transition is poorly known in this basin, the Buxières-les-Mines locality has always 115 116 been considered as Early Permian deposits (Roscher and Schneider, 2006; Schneider and 117 Werneburg, 2006; Steyer et al., 2000). Correlated with the lower 'Autunian' local age (Debriette, 1992; Stever et al., 2000), the Buxières Formation extends from the latest Asselian 118 to the Middle Sakmarian, (Roscher and Schneider 2006; Schneider and Werneburg 2006). Its 119 120 geological age remains to be refined; however, the volcanic tuffs 'Lien Blanc' and 'Lien Vert' have been radiometrically dated at 294.6 ± 3.2 Ma (Ducassou et al., 2018) and at 121 approximatively 298 Ma (M. Mercuzot, pers. comm., 2023), respectively, which implies an 122 early to late Asselian age for this locality. The palaeoenvironment of Buxières-les-Mines 123 could represent lacustrine or palustrine environments, which experienced several drying 124

events (Kaulfuß, 2003) without direct evidence of marine influences, contrary to Schultze and
Soler-Gijón's (2004) and Schultze's (2009) opinions for all the basins of the Northern Massif
central.

The Autun Basin is a half-graben basin, oriented West-East, located in the Northern Massif central (Fig. 1B; Saône-et-Loire, France; Gand et al., 2015, 2017). It is divided into four formations: Igornay and Muse formations constituting the lower 'Autunian' (upper Gzhelian to lower Asselian), and Surmoulin and Millery formations corresponding to the upper 'Autunian' (post-Assselian; Pruvost, 1942). The basin is interpreted as representing fluvio-lacustrine environments (Pruvost, 1942; Marteau, 1983; Mercuzot, 2020; Mercuzot et al., 2022).

The Muse OSB is located in the Muse Formation (Gand et al., 2011, 2015, 2017; Pellenard et al., 2017). It is mainly composed of oil-shale beds with intercalations of volcanic tonsteins (Fig. 1E). Two tonsteins were radiometrically dated at 298.05 \pm 0.39 Ma and 298.57 \pm 0.38 Ma (upper part of the Muse OSB stratigraphy in Pellenard et al. [2017]). The Muse OSB is therefore dated as lower Asselian (lowermost Permian) in age. Mercuzot (2020) assigned the sedimentary deposits to a palustrine environment that corresponds to a coastal freshwater lake.

142

143 **3. Material and methods**

144 3.1. $\delta^{18}O_p$ analysis

Bioapatite samples were treated following a previously described wet chemistry protocol (Crowson et al., 1991; Lécuyer et al., 1993). This protocol consists of the isolation of the phosphate ions (PO_4^{3-}) from bioapatite using acid dissolution and anion-exchange resin and precipitated as silver phosphate (Ag₃PO₄) crystals. For each sample, between 10 and 30 mg of dentine powder was dissolved in 2 ml of 2 M HF for 24hrs. The CaF₂ residue was separated by centrifugation and the solution was neutralized by adding 2.2 ml of 2 M KOH.

AmberliteTM IRN 78 anion-exchange resin (2.5 ml) was added to the solution to separate the PO₄³⁻ ions. After 24 h, the solution was rinsed with deionized water and the resin was eluted with 27.5 ml of 0.5 M NH₄NO₃. After 4 h, 0.5 ml of NH₄OH and 15 ml of an ammoniacal solution of AgNO₃ were added and the samples were placed in a thermostated bath at 68°C for 7 h, allowing the precipitation of Ag₃PO₄ crystals.

Oxygen isotope compositions were measured using a high-temperature pyrolysis 156 technique involving a VarioPYROcube™ Elemental Analyser (Elementar GmbH) based on 157 'purge and trap' technology interfaced in Continuous Flow mode with an Isoprime[™] Isotopic 158 Ratio Mass Spectrometer (Elementar UK Ltd) using the protocol described in Fourel et al. 159 (2011). For each sample, 5 aliquots of 300 µg of Ag₃PO₄ were mixed with 400 µg of carbon 160 black powder and loaded in 3.5x5 mm silver foil capsules. Pyrolysis was performed at 161 1450°C. Measurements were calibrated against NBS120c (natural Miocene phosphorite from 162 Florida) and NBS127 (barium sulfate, BaSO₄). The certified δ^{18} O value of NBS120c was 163 fixed at 21.7% (Lécuyer et al., 1993; Halas et al., 2011) and the δ^{18} O of NBS127 set at the 164 certified value of 9.3‰ (V-SMOW; Hut, 1987) for calibration of the unknown silver 165 phosphate samples. Silver phosphate samples precipitated from standard NBS120c were 166 repeatedly analysed ($\delta^{18}O_p = 21.7\%$; $1\sigma = 0.2$; n = 20) along with the silver phosphate 167 168 samples derived from fossil bioapatites to ensure that no isotopic fractionation occurred during the wet chemistry. In this manuscript we have used the classical "permil" notation 169 (‰). For ¹⁸O/¹⁶O delta notation, the reference was V-SMOW. $\delta^{18}O_p$ notation means delta 170 notation versus V-SMOW for phosphate samples. 171

172

173 3.2. $\delta^{18}O_c$ and $\delta^{13}C_c$ analyses

To remove potential organic contaminants and secondarily precipitated calcite,
bioapatite samples were pre-treated following the protocol of Koch et al. (1997). About 10 mg

of bioapatite powder was washed with a 2% NaOCl solution, followed by a 0.1 M acetic acid
solution. Each treatment lasted for 24 h and samples were rinsed 5 times with distilled water
between treatments. Pre-treated powders were collected after 24 h of air-drying at 40°C.

Carbon and oxygen isotope compositions were measured using an isoFLOW[™] system 179 connected on-line in continuous flow mode to a precisIONTM mass spectrometer (Elementar 180 UK). For each sample, three aliquots of 1 to 2 mg of pre-treated bioapatite powder were 181 182 loaded in LABCO Exetainer® 3.7 ml soda glass vials, round bottomed with Exetainer caps, and were reacted with anhydrous phosphoric acid. The reaction took place at 90°C in a 183 temperature regulated sample tray. The CO₂ gas generated during the acid digestion of the 184 carbonate sample was then transferred to the mass spectrometer via the centrION[™] interface. 185 Calibrated CO₂ gas was used as the monitoring gas. For bioapatite, the acid fractionation 186 factor α (CO₂-apatite carbonate) of 1.00773 determined for the NBS120c phosphate rock 187 188 reference material was used (Passey et al., 2007).

The calibrated materials used were Carrara marble ($\delta^{18}O_c = -1.84\%$, $\delta^{13}C_c = 2.03\%$; Fourel et al., 2016), NBS18 ($\delta^{18}O_c = -23.2\%$, $\delta^{13}C_c = -5.01\%$; Friedman et al., 1982; Hut, 1987; Stichler, 1995; Coplen et al., 2006) and NBS120c ($\delta^{18}O_c = -1.13\%$, $\delta^{13}C_c = -6.27\%$; Passey et al., 2007). Isotopic compositions are quoted in the standard δ notation relative to V-SMOW for oxygen and V-PDB for carbon.

194

195 3.3. $\delta^{34}S$ analysis

Sulfur isotope compositions of bioapatite samples were measured using a
VarioPYROcube[™] Elemental Analyser in NCS combustion mode based on 'purge and trap'
technology, interfaced in continuous-flow mode with an Isoprime[™] 100 Isotope Ratio Mass
Spectrometer. The technique is fully described in Fourel et al. (2014). Bioapatite samples
were analysed by weighing 3 aliquots of 5 mg of untreated apatite in tin foil capsules mixed

with 15 mg of pure tungsten oxide (WO₃) powder. Tungsten oxide is a powerful oxidant that
ensures the full thermal decomposition of bioapatite sulfate into sulfur dioxide (SO₂) gas
(Goedert et al., 2016).

Measurements were calibrated against IAEA-S-2 (silver sulfide, Ag₂S; δ^{34} S = 22.7‰; 204 Stichler, 1995), IAEA-SO-5 (barium sulfate BaSO4; δ^{34} S = 0.5‰; Halas and Szaran 2001), 205 and IAEA-SO-6 (barium sulfate BaSO4; $\delta^{34}S = -34.1\%$; Halas and Szaran 2001), 206 international standards (Halas and Szaran, 2001). For each analytical run of bioapatite 207 samples, we have also analysed BCR32 samples as a compositional and isotopic standard (S% 208 = 0.72, certified value; δ^{34} S = 18.4‰; Fourel et al., 2015; Goedert et al., 2016) to ensure that 209 210 analytical conditions were optimal to perform sulfur isotope analyses on samples with lowsulfur content. The standard deviation of δ^{34} S measurements was better than 0.2‰. The 211 VarioPYROcubeTM Elemental Analyser is equipped with a Thermal Conductivity Detector 212 (TCD) and was used to measure the sulfur content of the samples. For ${}^{34}S/{}^{32}S$ delta notation. 213 the reference was V-CDT. 214

215

216 *3.4. Palaeotemperatures*

217 In primarily non-air-breathing vertebrates, the body temperature (T_b) is assumed to be 218 similar to that of the surrounding water (T_w) (e.g. Haesemeyer, 2020). However, some large and active pelagic fishes, such as lamnid sharks, billfishes, tunas and oar fishes, are able to 219 maintain higher T_b than their T_w (e.g. Carey and Teal, 1969; Goldman, 1997) as an adaptation 220 to their high energy demands to perform long migration or move in the column water. 221 However, the small sized aquatic vertebrates investigated in this study do not exhibit 222 anatomical characters that correspond to this specific ecology. Moreover, xenacanths have 223 been interpreted as potential fast-start swimmer like garpikes (Luccisano et al., 2021). 224 Consequently, we consider that Xenacanthiformes, Acanthodii and Actinopterygii from 225

Buxières-les-Mines and the Muse OSB are assumed to have their T_b similar to that of their T_w. Furthermore, the δ^{18} O value of their body water ($\delta^{18}O_{bw}$) is considered to be equal to the δ^{18} O of ambient environment ($\delta^{18}O_w$) (Kolodny et al., 1983). In order to investigate the T_b, we use the fractionation equation adapted from the phosphate-water temperature scale established by Lécuyer et al. (2013) that relates the bioapatite phosphate $\delta^{18}O_p$ value to that of body water and body temperature and that is valid for a large range of aquatic vertebrates:

232

233
$$T_b(^{\circ}C) = 117.4(\pm 9.8) - 4.5(\pm 0.43) \times (\delta^{18}O_p - \delta^{18}O_{bw})$$

234

```
235 3.5. Sampling
```

All the material comes from Buxières-les-Mines and the Muse OSB. We have chosen to investigate the dorsal spines of Xenacanthiformes because they are heavily mineralized structures composed of dentine (Reif, 1978), which is known for being able to well-preserve isotope signals (e.g. Fischer et al., 2013). Furthermore, they are non-replaced structures with a continuous growth (Soler-Gijón, 1999; Beck et al., 2016) that allow variations in the isotope composition to be tracked during the lifespan of these organisms.

The xenacanthiform dorsal spine growth pattern (Fig. 2) has been discussed by Soler-242 Gijón (1999) and Beck et al. (2016). They showed that the growth took place by the addition 243 of new proximal dentine layers. Thus, the oldest part of the dorsal spine is the apex, i.e. the 244 interior of the distal part. As the pattern of the different growth layers of the xenacanthiform 245 dorsal spines was not well-preserved, we sampled cf. Triodus sp. dorsal spines by cutting 246 small sections all along the length of each spine in order to collect large enough amounts of 247 bioapatite for the geochemical analyses (Fig. 2). For the cf. Orthacanthus sp. dorsal spine, we 248 followed a similar protocol focusing on the most external part of the spine to minimise mixing 249 of several growth layers (Fig. 2). 250

Following Jerve et al. (2017), the growth model of the acanthodian fin spines is more related to chondrichthyans than to osteichthyans, even though dentine growth layers were not identified in some extant (e.g. Maisey, 1979; Burrow et al., 2015, 2016) or extinct chondrichthyans (e.g. Maisey, 1978, 1982; Soler-Gijón, 1999; Beck et al., 2016). The acanthodian fin spine grows by implementation of new dentine material from the apex to the base. Consequently, the distal part of the fin spine is older than the base.

257

258 **4. Results**

259 *4.1. Stable isotope values*

The mean oxygen, carbon and sulfur isotope compositions of bioapatite phosphates and carbonates of each specimen are reported in Table 1 (see Table S1 for the detailed values of each sample). In the Muse OSB, the $\delta^{18}O_p$ values range from 17.3‰ to 25.1‰, the $\delta^{13}C_c$ from 3.3‰ to 5.9‰ and the $\delta^{34}S$ from 1.2‰ to 6.9‰. In Buxières-les-Mines, the $\delta^{18}O_p$ values range from 14.0‰ to 18.7‰, the $\delta^{13}C_c$ from –2.7‰ to 5.7‰ and the $\delta^{34}S$ from –20.3‰ to 7.9‰. Between the taxonomic groups, the temnospondyls from Buxières-les-Mines have the lowest $\delta^{18}O_p$ (15.1±0.6‰) and $\delta^{13}C_c$ (–2.6±0.1‰) values.

267

268 4.2. Isotopic variations along the spines

 $\delta^{18}O_p$ values of cf. *Triodus* sp. (Fig. 3A) dorsal spines from the Muse OSB range from 269 17.3‰ to 25.1‰. Different trends of the $\delta^{18}O_p$ values are observed along the dorsal spine 270 length. One dorsal spine (965a) shows no significant variations of the $\delta^{18}O_p$ values. For the 271 three other ones, there is an increase in $\delta^{18}O_p$ values from the apex to the base. Specimen 943 272 shows an increase of almost 2‰ and of more than 4‰ in specimens 326 and 907b. For the 273 two cf. Orthacanthus sp. dorsal spines from Buxières-les-Mines (Fig. 3B), $\delta^{18}O_p$ values range 274 from 17.2% to 18.0% (D13) and from 16.2% to 17.1% (BX04). The $\delta^{18}O_p$ values tend to 275 decrease from the apex to the base, they never exceed more than 18‰ and there is less than 276

1‰ difference between the highest and the lowest values. $\delta^{18}O_p$ values of cf. *Triodus* sp. from Buxières-les-Mines (Fig. 3C) range from 15.9‰ to 18.6‰. Despite increasing (BX28) or decreasing (D08), the $\delta^{18}O_p$ values within each dorsal spine do not vary more than 1‰ from the apex to the base, excepted for two spines (D07 and D11). The latter and one cf. *Orthacanthus* sp. (BX04) show a distinct decrease in $\delta^{18}O_p$ values in the distal half that can reach more than 1‰ in D11.

In Buxières-les-Mines, $\delta^{13}C_c$ values of BX04 range from 0.9‰ to 1.9‰ with the exception of the most proximal point (base of the dorsal spine) at almost 0‰ (Fig. 4B). The variation seems to be cyclical. $\delta^{13}C_c$ values of D08 continuously decrease from the apex to the base from 5.2‰ to 2.7‰. The $\delta^{34}S$ values of BX04 (Fig. 5) range from -6‰ to 3.8‰ following irregular cycles of decreases and increases with the highest values at the base of the dorsal spine. For the other xenacanth and acanthodian spines (Fig. 5), the $\delta^{34}S$ values decrease from the apex to the base.

Along the length of a same fin spine, the acanthodians from the Muse OSB and Buxières-les-Mines do not show significant variations in their $\delta^{18}O_p$ (Fig. 6), $\delta^{13}C_c$ (Fig. 4A) and $\delta^{34}S$ values (Fig. 5), i.e. less than 1‰. The only exception is the specimen (1924) from the Muse OSB, in which the $\delta^{18}O_p$, $\delta^{13}C_c$ and $\delta^{34}S$ values decrease from the apex to the base.

295

296 **5. Discussion**

297 5.1. Preservation of the original isotopic compositions of fossil bioapatite

No method is available to formally demonstrate that the original isotopic composition of the $\delta^{18}O_p$ is preserved in fossil bioapatite. However, several tests have been proposed. In modern vertebrate skeletal tissues, and supposedly in fossil ones, phosphates and carbonates of the bioapatite both precipitate near isotopic equilibrium with body water. Consequently, $\delta^{18}O_p$ and $\delta^{18}O_c$ are positively correlated. Re-equilibration of both phosphate and carbonate

303	with diagenetic fluids is not expected because both have different isotopic exchange rates.
304	Moreover, it is expected that the δ^{18} O values of phosphate and associated apatite-bound
305	carbonate of fossil fishes and sharks follow the same trend observed in modern sharks and
306	mammals (e.g. Kolodny and Luz, 1991; Bryant et al., 1996; Iacumin et al., 1996; Vennemann
307	et al., 2001; Lécuyer et al., 2003). $\delta^{18}O_p$ and $\delta^{18}O_c$ values of vertebrates from Buxières-les-
308	Mines and the Muse OSB follow the distribution of modern and fossil sharks (Fig. 7). In
309	addition, the intra-site variability is congruent with the known measured biological variability
310	of the $\delta^{18}O_p$ values in modern shark teeth (Vennemann et al., 2001). Re-crystallisation and
311	diagenetic effect on dentine tissues should result in a homogenisation of the values, not
312	observed in Buxières-les-Mines and the Muse OSB.
313	Another evidence in favour of an original preservation of the $\delta^{18}O_p$ values is the
314	difference of almost 1.5‰ between exclusive aquatic (fishes) and semi-aquatic (amphibians)
315	vertebrates in Buxières-les-Mines (Table 1). As they have different physiologies and
316	ecologies, this difference is expected because of the different origin of their body water. For
317	these reasons, we can consider that the original oxygen isotopic signal could be preserved. We
318	compared the oxygen isotope composition of the $\delta^{18}O_p$ and the $\delta^{18}O_c$ values with the
319	carbonate content (CO ₃ ^{2–} wt%) of each sample (Fig. 8). In modern sharks, the $\delta^{18}O_p$ values
320	can increase to 14.7‰ compared to the $\delta^{18}O_c$ values (Vennemann et al., 2001). Microbially-
321	induced diagenetic alteration has previously been shown to increase the offset between $\delta^{18}O_p$
322	and $\delta^{18}O_c$ values (e.g. Zazzo et al., 2004). The $CO_3{}^{2-}$ wt% values of teeth and bones of
323	modern vertebrates range from 2 to 13.4 wt% (Brudefold and Soremark, 1967; Rink and
324	Schwarcz, 1995; Vennemann et al., 2001). The samples from Buxières-les-Mines and Muse
325	OSB have $\delta^{18}O_c - \delta^{18}O_p$ and CO_3^{2-} wt% values (see Table S1 for the detailed values) out of the
326	supposed diagenetic area, except for two samples. The latter, at 5.9 wt% and 7.7 wt%
327	respectively, are clearly outside the 0.4 wt% to 3.3 wt% range of the other values. Thus, we

assume that the oxygen and carbon isotope compositions of apatite carbonate preserved theoriginal isotopic signal of the sampled data set.

The principal argument for the preservation of the isotopic composition of the $\delta^{13}C_c$ is 330 the systematic and significant difference of at least 3% in $\delta^{13}C_c$ values between fish and 331 amphibians in Buxières-les-Mines (Table 1). In the semi-terrestrial amphibians, the $\delta^{13}C_c$ 332 values mainly may reflect those of the diet. In this case, the isotope fractionation depends on 333 the digestive physiology (Passey et al., 2005). A contrario, for the fishes, the relationship 334 between the $\delta^{13}C_c$ values and diet is influenced by significant amounts of carbon deriving 335 from dissolved inorganic carbon of the ambient water (McConnaughey et al., 1997, Thorrold 336 et al., 1997), resulting in higher $\delta^{13}C_c$ values (Santos et al., 2011). 337 As far as the δ^{34} S values are concerned, secondary minerals can precipitate at the 338 surface or within the bones during fossilisation and they would tend to increase the sulfur 339 340 content of bones, which is lower than 0.6 weight% S (wt% S) in modern bioapatite (e.g. Goedert et al. 2018). The Muse OSB samples show globally lower wt% S (mean of 0.4 wt%) 341 S) than those of Buxières-les-Mines (mean of 1.1 wt% S). In the Muse OSB, acanthodians and 342 actinopterygians have similar δ^{34} S values and sulfur contents that vary in a narrow range 343 within each taxonomic groups (Fig. 9). In Buxières-les-Mines, the sample size is higher than 344 345 in the Muse OSB. Consequently, for each common taxonomic groups, the variability in the δ^{34} S and wt% S values is higher in Buxières-les-Mines than in the Muse OSB (Fig. 9). 346 However, the main part of the data ranging from -10% to 10% for δ^{34} S and from 0.1 wt% S 347

to 2 wt% S for the sulfur content. Within temnospondyls and xenacanths, a few points show

low δ^{34} S values for slightly higher wt% S. Consequently, these few samples are interpreted as

diagenetically altered, whereas the remaining δ^{34} S measurements of Buxières-les-Mines are

351 interpreted as reflecting the living environment of the studied vertebrates.

5.2. Palaeoenvironmental reconstruction of Buxières-les-Mines and the Muse OSB
5.2.1. δ³⁴S

Seawater δ^{34} S value was close to 12‰ at the Carboniferous-Permian transition (Claypool et al., 1980), highly contrasting with the modern δ^{34} S value of 20.99±0.25‰ (Rees et al., 1978; Paytan et al., 2020). Based on recent investigations conducted on modern and fossil vertebrates from a broad phylogenetic context (Goedert, 2017; Goedert et al., 2018, 2020), the δ^{34} S value of vertebrate bioapatite is supposed to be close to that of their living environment in the absence of sizable isotopic fractionation (0.5±2.4‰) between the animal and its diet (Nehlich, 2015).

All the taxonomic groups from Buxières-les-Mines exhibit δ^{34} S values lower than 362 12‰ with variations from –6.0‰ to 9.6‰ for unaltered samples. The δ^{34} S values from the 363 Muse OSB range from 1.2‰ to 6.9‰. Those samples are depleted in heavy isotope by at least 364 365 3‰ and on average by 10‰ compared to seawater. This means that their sulfur content is mainly derived from river input. To a lesser extent, brackish water could have influenced the 366 three highest δ^{34} S values from Buxières-les-Mines: 9.6‰ for an actinopterygian and 7.1‰ 367 and 7.9% for two temnospondyls. In light of the bioapatite δ^{34} S values, the environment of 368 Buxières-les-Mines and the Muse OSB do not seem to have been subjected to significant 369 370 marine influences contrary to what was assumed in previous studies (e.g. Schultze and Soler-Gijón 2004; Schultze, 2009). 371

372

373 5.2.2. $\delta^{18}O_p$

Conodont $\delta^{18}O_p$ values are considered to be relevant proxies of seawater temperatures during the Palaeozoic (Joachimski et al., 2004, 2006, 2009; Trotter et al., 2008; Wenzel et al., 2008; Chen et al., 2013). Consequently, we can consider that $\delta^{18}O_p$ values of the Early Permian marine setting is close to 22‰ according to Chen et al. (2013). We therefore do not

agree with Fischer's et al. (2013) opinion who considered 18‰ as the lower limit for the $\delta^{18}O_p$ values of the Early Permian marine setting.

In Buxières-les-Mines, except for the temnospondyls, which have $\delta^{18}O_p$ values between 14.0‰ and 15.7‰, the aquatic vertebrate fauna, i.e. actinopterygians, acanthodians and xenacanthiforms, have $\delta^{18}O_p$ values ranging from 15.7‰ to 18.7‰ (Table S1). These values indicate a freshwater environment. Furthermore, highest $\delta^{18}O_p$ values, close to 19‰, are not positively correlated with $\delta^{34}S$ values (see Table S1), so that any potential marine influence is unlikely.

Strict aquatic vertebrates are supposed to be part of the same food web (Kriwet et al., 386 2008), but this does not mean that they share the same $\delta^{18}O_p$ values. There could be vertical 387 water temperature gradients in lakes even if it is less marked in temperate lakes than in 388 tropical ones (Lewis Jr, 1987). Temnospondyls have $\delta^{18}O_p$ values almost 2‰ lower than those 389 390 measured in the other taxa of the faunal association (Table 1). This observation is congruent with an ecological partitioning due to their semi-terrestrial behaviour. Palynomorph 391 assemblages indicate coal-swamp to mesoxerophytic environments, indicating the prevalence 392 of humid conditions, at least at a seasonal scale (Paquette et al., 1980; Steyer et al., 2000). 393 Therefore, temnospondyls could partly live in a humid tropical environment characterised by 394 precipitation slightly or not ¹⁸O-depleted relative to the global ocean. Another explanation 395 could be provided by a high-altitude habitat where the depletion in heavy isotopes of waters 396 increase with the related decrease in air temperature (Dansgaard, 1964). As modern giant 397 398 salamanders can live up to 1,500 meters above sea level (Gang et al., 2004), it cannot be excluded that temnospondyls may have occupied similar habitats. To the contrary, the $\delta^{18}O_p$ 399 values of aquatic taxa could derive from the lake water, which is under evaporation 400 influences, and thus, had higher water δ^{18} O values. Consequently, the δ^{18} O_p values derived 401 from precipitations exhibit lower values than those derived from lake water. 402

403	In the Muse OSB, the $\delta^{18}O_p$ values range from 17.3‰ to 25.1‰ for xenacanthiforms,
404	from 19.3‰ to 21.3‰ for acanthodians and from 17.6‰ to 18.6‰ for actinopterygians. As
405	for Buxières-les-Mines, most of them, lower or close to 22‰, can be interpreted as freshwater
406	markers. However, the mean $\delta^{18}O_p$ value in the Muse OSB is higher (20.0‰) than that of
407	Buxières-les-Mines (17.0‰) and numerous $\delta^{18}O_p$ values, especially in xenacanthiforms and
408	acanthodians, are higher than 22‰ and up to 25.1‰. Permian conodont $\delta^{18}O_p$ is in the range
409	of 21‰–23‰ and match some $\delta^{18}O_p$ values recorded in the Muse OSB. However, high $\delta^{18}O_p$
410	may reflect ¹⁸ O-enriched water due to large evaporation rates that commonly take place in
411	arid environments. Such mechanisms can be favoured by monsoonal climates, which were
412	supposed to occur in these low latitude tropical basins as postulated by Roscher and Schneider
413	(2006) based on Parrish's (1993) and Kutzbach and Ziegler's (1994) modelling. Shallow
414	tropical waters, such as swamps, lagoons or lakes, are characterised by a dry and a humid
415	season, both being warm with a contrasted hydrological budget leading to $\delta^{18}O_p$ differences in
416	the aquatic vertebrate fauna of up to 5‰ (Otero et al., 2010), which are in the range of the
417	highest $\delta^{18}O_p$ values compared to the lowest ones. The highest $\delta^{18}O_p$ values are higher than
418	those of the contemporaneous marine vertebrates and no sedimentological,
419	palaeogeographical or geochemical (present $\delta^{34}S$ analyses) evidence agrees with a potential
420	connection between the French Massif central basins and a marine environment. We therefore
421	interpret the Muse OSB as a shallow freshwater environment recording extensive drying
422	events.
423	

423

424 5.2.3. $\delta^{13}C_c$

425 The $\delta^{13}C_c$ values of aquatic vertebrates of Buxières-les-Mines and the Muse OSB 426 range from -0.8‰ to 7.0‰. These values are globally different from those recorded by the 427 modern marine shark teeth. In the latter, $\delta^{13}C_c$ values range from -6.8‰ to 4.8‰

(Vennemann et al., 2001). Previous studies devoted to fossil and modern fishes (see Kolodny 428 429 and Luz, 1991; Fricke et al., 1998; Vennemann et al., 2001; Amiot et al., 2010; Błażejowski et al., 2013; Goedert et al., 2016) showed that the $\delta^{13}C_c$ values of the apatite of freshwater and 430 marine vertebrates can overlap and are not a good proxy for discriminating these two 431 environments. However, Horton et al. (2015) showed, based on water evaporation 432 experiments performed in the laboratory, that an unambiguous ¹³C-enrichment occurs with an 433 increase of aridity factor, i.e. precipitation:evaporation. Consequently, the high $\delta^{13}C_c$ values 434 of the aquatic vertebrates from Buxières-les-Mines and the Muse OSB could be related to 435 extensive drying events occurring in an arid environment. This is congruent with the 436 interpretation of the $\delta^{18}O_p$ values. 437

 $\delta^{13}C_c$ of temnospondyls are lower than those of strict aquatic taxa, with an average of 438 -2.6% with low variability (sd = 0.1). Again, these values could be interpreted as ecological 439 partitioning but not due to their semi-terrestrial way of life. In fact, during the late Palaeozoic 440 (e.g. Davies et al., 2012), the marine organic matter had lower δ^{13} C values than the terrestrial 441 one, contrary to the present day (e.g. Clementz and Koch, 2001). The observed difference 442 between the temnospondyls and the aquatic vertebrates, ranging from 2‰ to 5‰, could be 443 caused by different life habits. As the high $\delta^{13}C_c$ values of aquatic vertebrates are evidence for 444 an arid environment linked to extensive water evaporation, the lower $\delta^{13}C_c$ values of 445 temnospondyls could reflect an opposite process. When the palaeo-lake in Buxières-les-Mines 446 experienced arid conditions, temnospondyls could be able to move to more humid 447 448 environments being less influenced by water evaporation, like a humid forest. This is congruent with modern amphibians that avoid arid environments (Zancolli et al., 2014) and 449 the ecological hypothesis of $\delta^{18}O_p$ values that postulated a life partly in a tropical humid forest 450 for the temnospondyls of Buxières-les-Mines. 451

453 *5.2.4. Reconstruction of palaeotemperatures*

454 Water palaeotemperatures were calculated using the phosphate-water temperature equation of Lécuyer et al. (2013), and using the $\delta^{18}O_w$ values of five different modern aquatic 455 environments as possible analogues to those of the Muse OSB and Buxières-les-Mines where 456 the vertebrates lived (Fig. 10; see Table S2 for detailed values): seawater with (0‰) and 457 without (-1‰) glaciation (Shackleton, 1975), Lake Matano (-4.3‰; Katsev et al., 2010), 458 459 Lake Punta Laguna (0.93%; Curtis et al., 1996) and Lake Tanganyika (3.85%; Casanova and Hilaire-Marcel, 1992) in order to find the most theoretically viable value. 460 For Buxières-les-Mines, the calculated palaeotemperatures (Fig. 10) range from 461 462 34±0.5°C to 44±0.2°C and from 29±0.5°C to 40±0.2°C for the seawater models with and 463 without glaciation respectively, from 14±0.5°C to 25±0.2°C for the Lake Matano model, from 38±0.5°C to 48±0.2°C for the Lake Punta Laguna model and from 52±0.5°C to 62±0.2°C for 464 465 the Lake Tanganyika model. For the Muse OSB, the palaeotemperatures (Fig. 10) range from 9±5°C to 38.1±0.1°C and from 5±5°C to 33.6±0.1°C for the seawater models with and 466 without glaciation respectively, from -10±5°C to 18.8±0.1°C for the Lake Matano model, 467 from 13±5°C to 42.3±0.1°C for the Lake Punta Laguna model and from 27±5°C to 468 469 55.9±0.1°C for the Lake Tanganyika model. 470 The viable environmental temperatures of extant tropical actinopterygians range from

16°C to 40°C (Pandian and Vivekanandan, 1985) and those of freshwater stingrays from 25°C
to 33°C (Almeida et al., 2009). According to these viable modern temperature ranges, the
most viable palaeotemperature model, i.e. with temperatures between 14.4°C to 24.8°C (Fig.
10; Table S2), for Buxières-les-Mine is the Lake Matano, a tropical freshwater lake with a
significant depth (several hundred meters). The water budget of the Lake Matano is triggered
by a monsoon regime, i.e. with an alternation of dry and wet seasons. Moreover, aridity
events have been proposed at Buxières-les-Mines based on sedimentological facies analyses

(Kaulfuß, 2003). According to this body of knowledge, this Permian locality, as already
supposed, could have been a rather deep tropical palaeo-lake. This hypothetical aquatic
palaeoenvironment is also compatible with the documented faunal association extending from
small actinopterygians to large *Orthacanthus*, as well as temnospondyls (e.g. Steyer et al.,
2000). It is worth to note that such faunal diversity could not be present in small hydrological
systems because it would require a large aquatic environment like open lakes to develop and
to remain steady (Salzburger et al., 2014).

For the Muse OSB, the lowest $\delta^{18}O_p$ values agrees with viable temperature (Fig. 10) in a model similar to the Lake Punta Laguna model which is a shallow freshwater lake with only a few meters depth, so a good analogue to the coastal freshwater lake proposed by Mercuzot (2020) and Mercuzot et al. (2022). The presence of only small-sized animals supports the hypothesis of a shallow environment.

490

491 5.3. Palaeoecology of xenacanths and acanthodians

Along the *Orthacanthus* dorsal spine, $\delta^{13}C_c$ values vary cyclically (Fig. 4). The 492 apparent cycles whose amplitude does not exceed 1‰ could correspond to changes in the 493 water budget of the lake. However, the sole investigated cf. Triodus sp. (D08) shows a clear 494 decrease in the $\delta^{13}C_c$ values (3‰) from the apex to the base. The $\delta^{13}C_c$ decrease is positively 495 correlated to the $\delta^{18}O_p$ values in the same specimen (see Table S1). It has been demonstrated 496 that a $\delta^{13}C - \delta^{18}O$ covariation can occur in closed-basin lakes (e.g. Li and Ku, 1997; Horton et 497 al., 2015). Following our palaeoenvironmental reconstruction, Buxières-les-Mines therefore is 498 interpreted as a closed-basin lake and the co-variation in $\delta^{13}C_c$ and $\delta^{18}O_p$ values could be 499 500 related to changes in the water level. Here, the decrease from the apex to the base could indicate that specimen D08 moved from a shallow environment to a deeper setting during its 501

lifespan, as it grew. This could be related to habitat partitioning between juveniles (shallow
environment) and adults (deeper environment) as in modern sharks (DeAngelis et al., 2008).
The variation in the δ¹⁸O_p values along the acanthodian spines from Buxières-lesMines (Fig. 6) does not exceed more than 0.5‰, which could correspond to known
temperature variations, i.e. up to 2°C, in modern tropical lakes (Lewis Jr, 1987).
Consequently, the living environment of acanthodians seems to have remained quite the same
all along their lifes.

Similar conclusions are inferred from the xenacanths from Buxières-les-Mines with $\delta^{18}O_p$ variations that also do not exceed 1‰ (Fig. 3C). However, the variation pattern differs to that of acanthodians. In four specimens, a distinct decrease is reported and reach up to 1.5‰ in specimen D11. As the observed values are lower than 22%, they could be related to changes in water supply caused by wet and dry seasons as already proposed for this locality (Kaulfuß, 2003).

The $\delta^{18}O_p$ variation along the acanthodians fin spines from Muse OSB is negligible 515 (sd=0.1) for one spine (1955) and more variable in another one (1924) with a significant 516 decrease from the apex to the base. Spine 1955 has values ranging from 19% to 20%, while 517 those of spine 1924 vary from 20% to more than 21%. These $\delta^{18}O_p$ values show that the 518 acanthodians could live in variable environments and were able to endure drying periods. A 519 δ^{13} C– δ^{18} O covariation is observed in specimen 1924 (see Table S1) as observed in xenacanths 520 from Buxières-les-Mines. The δ^{13} C and δ^{18} O values decrease in the same way from the apex 521 to the base, suggesting once again changes in the hydrological budget. 522

This ability to live in a shallow low-oxygenised environment was already proposed for xenacanthiforms based on morphological arguments (e.g. Compagno, 1990). In the Muse OSB, the dorsal spines with the most variable $\delta^{18}O_p$ values are also those with the highest $\delta^{18}O_p$ values (Fig. 3A). This could be evidence for the ability of xenacanthiforms to live in

shallow freshwater environments submitted to high hydrological variations like periods of

drying. This interpretation follows Mercuzot's (2020) and Mercuzot et al.'s (2022)

529 conclusions in considering Muse OSB as a shallow and coastal lake, i.e. with a depth of only530 a few meters.

The variations in δ^{34} S continuously decrease in the investigated cf. Acanthodes sp. and 531 cf. Triodus sp. specimens, contrary to what is observed in cf. Orthacanthus sp (Fig. 5). The 532 δ^{34} S value of the environmental water vary in response to changes in river runoff (δ^{34} S = 0– 533 10%; Krouse, 1980), volcanic inputs (δ^{34} S \approx 0%; Paytan et al., 2020), and deposition of 534 evaporite minerals (δ^{34} S $\approx 21\%$) or sedimentary iron sulfides such as pyrite (δ^{34} S = -15%; 535 536 Krouse, 1980; Kaplan, 1983). Buxières-les-Mines and the Muse OSB could have been two intra-mountainous lacustrine systems submitted to intense river runoff due to their 537 palaeogeographical location in the Hercynian Mountains. Moreover, the basins of the French 538 539 Massif central were exposed to a recurrent volcanic activity as attested by the presence of tonsteins and ash levels documented in the sedimentary deposits of the two studied localities 540 (e.g. Steyer et al., 2000; Pellenard et al., 2017). Consequently, the observed $\delta^{34}S$ variation 541 within the xenacanth and acanthodian spines could reflect a combination of such 542 environmental fluctuations. 543

544

545 *5.4. Trophic and food web*

546 Considering that the $\delta^{13}C_c$ values reflect those of organic matter before the 547 mineralization process in the vertebrate skeleton, the $\delta^{13}C_c$ of predators is expected to be 548 higher by almost 1‰ relative to their potential preys (e.g. Cerling and Harris 1999). This 549 pattern of isotopic enrichment within the trophic chain could be indeed recorded in the $\delta^{13}C_c$ 550 of acanthodians, actinopterygians and the small xenacanthid *Triodus*. It is therefore surprising 551 that the large diplodoselachid *Orthacanthus* has such low $\delta^{13}C_c$ values (from -0.4‰ to 1.9‰).

Boy and Schindler (2000) and Kriwet et al. (2008) proposed that the large Orthacanthus was 552 553 the apex predator of its ecosystem, feeding on all the other smaller predators such as Triodus and temnospondyls. Indirect evidence of consumption of Triodus by Orthacanthus in the 554 Puertollano Basin (Gzhelian of Spain) was reported by Soler-Gijón (1995) and temnospondyl 555 mandible with an Orthacanthus tooth stuck in it was reported from Buxières-les-Mines (Fig. 556 557 11). It is therefore probable that, in Buxières-les-Mines, Orthacanthus preyed on Triodus and temnospondyls too. The Orthacanthus $\delta^{13}C_c$ values are intermediate between those of Triodus 558 and temnospondyls. If Orthacanthus preved on these two taxa, these values are expected 559 because they reflect the diversity of its preys: Triodus evolving in strict aquatic environments 560 561 and temnospondyls evolving in a semi-terrestrial one.

562 The faunal composition of the investigated localities is compatible with the two proposed environmental interpretations (Fig. 12). In Buxières-les-Mines, many components of 563 564 the Carboniferous-Permian freshwater fauna were already reported in other basins like the Saar-Nahe Basin and its large lacustrine system (e.g. Kriwet et al., 2008). These observations 565 favour the hypothesis of an open, large and deep lake, in which the complete food web is 566 represented with large predators or tertiary consumers (Orthacanthus and temnospondyls), 567 568 small predators or secondary consumers (Triodus) and preys as well as small consumers or 569 primary consumers (acanthodians and actinopterygians). In the Muse OSB, the food web is 570 mainly limited to small consumers (acanthodians and actinopterygians) and small predators (Triodus). A systematic revision has shown that a large Orthacanthus was present in the Muse 571 572 OSB with O. cf. kounoviensis (Luccisano et al., 2022). The single reported lateral tooth does not reach the size of the large adult teeth of O. kounoviensis from Buxières-les-Mines, so it 573 574 could correspond to a medium-sized animal distinct from the very large Orthacanthus recovered from Buxières-les-Mines, or to a late juvenile or a sub-adult specimen. 575 576 Consequently, this shark could have been able to live in shallow as well as large lakes.

However, the presence of this single tooth in the Muse OSB could be questioned because its 577 578 stratigraphic origin is unclear. Even if it is supposed to come from the base of the Muse OSB (Luccisano et al., 2022), no Orthacanthus material was found during recent excavation 579 campaigns (Gand et al., 2011, 2015; and during the last campaign in 2021). As the Muse OSB 580 presents a distinct East-oriented dip and the provenance of the tooth is unclear according to 581 Heyler (1969), this tooth could come from a different stratigraphic level older or younger than 582 583 the analysed material. In the light of our results, the Muse OSB fauna is more likely to be 584 related to a small and shallow aquatic environment than to open and large lakes or riverchannels. 585

586

587 5.5. Implication for the palaeobiogeography of the xenacanths at the Carboniferous-Permian
588 transition

589 Our analyses also show a differential environmental adaptiveness among the Xenacanthiformes of the Early Permian. The large Diplodoselachidae were restricted to large 590 and deep lakes and river systems like Buxières-les-Mines in France whereas the small 591 Xenacanthidae were able to inhabit more diversified environments, ranging from large lakes 592 593 to shallow swamps like in the Muse OSB. The observed different ecologies fit in with the 594 current known palaeobiogeography of the Carboniferous-Permian Xenacanthiformes from Europe. The large xenacanthiforms like *Orthacanthus* are almost restricted to the upper 595 Carboniferous in which large freshwater basins in connection with each other were present 596 597 (e.g. Luccisano et al., 2022). At the Carboniferous-Permian transition, the Francovian tectonic motions suppressed the connections between large basins containing large and deep lakes like 598 599 Buxières-les-Mines (e.g. Schneider, 1996). The resulting isolated basins were of smaller size and contained smaller lacustrine systems like the Muse OSB. In such shallow lakes, only 600 small xenacanthiforms like *Triodus* were able to live, a scenario in compliance with the 601

apparent diversification of *Triodus* throughout the Early Permian. The large xenacanthiforms,
however, continued to exist in a few peculiar locations such as Buxières-les-Mines or the
Saar-Nahe Basin, in which large and deep lakes prevailed.

605

606 **6.** Conclusions

The oxygen, carbon and sulfur isotope compositions of aquatic vertebrate bioapatite 607 608 from two Early Permian localities of the French Massif central allow reconstructing their palaeoenvironment. The non-contemporaneous localities of the Muse OSB and Buxières-les-609 Mines accordingly represent two different aquatic environments. Buxières-les-Mines is a 610 611 large, open and deep freshwater lake containing a diversified vertebrate fauna, ranging from large xenacanthiforms to small actinopterygians. A contrario, the Muse OSB is a less 612 613 taxonomically diversified locality with only small sized vertebrates that lived in a shallow freshwater environment experienced periodic and intense drying events. These localities 614 illustrate the environmental changes of the aquatic setting of the Early Permian intra-615 616 mountainous basins of the European Hercynian Mountains. Buxières-les-Mines is a remnant 617 of the large lacustrine systems of the upper Carboniferous, in which diversified aquatic vertebrates occurred. It represents one of the last large lacustrine systems in the Early Permian 618 619 of Europe. The Muse OSB represents one of the most common intra-mountainous freshwater ecosystems occurring during the Early Permian. It contains a less diversified fauna than in 620 Buxières-les-Mines with vertebrates small in size evolving in shallow lakes or swamps, most 621 likely cyclically submitted to significant drying up events. This study also agrees with 622 previous analyses that postulated that these intra-mountainous basins were not submitted to a 623 624 significant marine influence during the Early Permian.

This palaeoenvironmental reconstruction revealed that Early Permian
Xenacanthiformes from France lived in a rather uniform freshwater environment with no or
restricted marine influences and without migrations into marine settings. However, small

xenacanthiforms were adapted to extreme conditions such as drying events or low oxygenated
waters. This adaptation could explain their diversification in the Early Permian. These
palaeoecological assumptions are contrary to those previously deduced from American
species. Further studies conducted at regional or global scales will be able to identify different
adaptive strategies within this group during their evolutionary history and to explain their
global distribution in the Late Palaeozoic.

634

635 Acknowledgements

The authors thank the Rhinopolis Association, the Buxières-les-Mines Town hall and 636 the Conseil Départemental de l'Allier for the funding of the excavation campaigns in 637 Buxières-les-Mines during which the studied specimens were recovered, and for providing 638 639 storage space in which the Buxières-les-Mines fossils are housed. They also thank the Muséum d'Histoire Naturel d'Autun (MHNA) and its curator Dominique Chabard for access 640 to the Muse OSB specimens. Specimens from the Muse OSB were found during several 641 642 excavation campaigns (2010-2014 and 2021) and the authors thank for their valuable help D. 643 Beaudoin, F. Beaudoin, R. Pillon, G. Barnay, P. Baudinaud, N. Pégon, B. Arnoult (SHNA), D. Chabard, E. Chabard, A. Margueron (MHNA), the Gevrey, Barnay, and Jacquemard 644 645 families, G. Grillot, S. Kunz (Dracy-Saint-Loup Municipality) B. Blanc (Marine), E. Chenal (Éducation Nationale), C. Delhaye (CNRS), I. van Waveren and her students (Naturalis, 646 Leiden), J. Fortuny (ICP, Barcelona), S. Hervet (PaléOvergne), J. Galtier (Montpellier), A. 647 Bercovici (Manchester University), F. Prost (Dijon University), S. Giner (Var Département), 648 K. Rey (ex-BPI), and J.-S. Steyer, O. Béthoux, G. Cousin, G. Odin, L. Anseaume, J. Barbier, 649 M. Sanders, D. Perez, J. Falconnet, D. Germain and V. Rouchon (MNHN). All the isotopic 650 analyses were performed at the Plateforme d'Écologie Isotopique of UMR 5023 LEHNA, 651 Université Claude Bernard Lyon 1, France, member of the RéGEF network. The first author 652

653	was funded by the Doctoral School ED 341 - E2M2 Évolution Écosystème Microbiologie
654	Modélisation, Université Claude Bernard Lyon 1, France.
655	
656	Authorship contribution statement
657	V. L., G.C., A.P., R.A. and C. L. designed the research. V.L., K. L., R. A. and F.F.
658	performed the analyses. V.L. wrote the original draft and prepared the figures and tables. J
659	M.P. made the material available and led the field work in Buxières-les-Mines. All authors
660	discussed, wrote and approved the manuscript.
661	
662	Data availability
663	All data are available in the supplementary materials and within the present article.
664	
665	Declaration of competing interest
666	The authors declare no conflict of interest.
667	
668	References
669	Almeida, M.P.D., Barthem, R.B., Viana, A.D.S., Charvet-Almeida, P., 2009. Factors affecting
670	the distribution and abundance of freshwater stingrays (Chondrichthyes:
671	Potamotrygonidae) at Marajó Island, mouth of the Amazon River. Pan-Am. J. Aquat.
672	Sci. 4, 1–11.
673	Amiot, R., Wang, X., Lécuyer, C., Buffetaut, E., Boudad, L., Cavin, L., Ding, Z., Fluteau, F.,
674	Kellner, A.W.A., Tong, H., Zhang, F., 2010. Oxygen and carbon isotope compositions
675	of middle Cretaceous vertebrates from North Africa and Brazil: ecological and
676	environmental significance. Palaeogeogr. Palaeoclimatol. Palaeoecol. 297, 439-451.
677	Beck, K.G., Soler-Gijón, R., Carlucci, J.R., Willis, R.E., 2016. Morphology and histology of
678	dorsal spines of the xenacanthid shark Orthacanthus platypternus from the Lower

679	Permian of Texas, USA: Palaeobiological and palaeoenvironmental implications. Acta
680	Palaeontol. Pol. 61, 97–117.

- Błażejowski, B., Duffin, C.J., Gieszcz, P., Małkowski, K., Binkowski, M., Walczak, M.,
- 682 Mcdonald, A.A., Withers, P.J., 2013. *Saurichthys* (Pisces, Actinopterygii) teeth from
- the Lower Triassic of Spitsbergen, with comments on their stable isotope composition
- 684 (δ^{13} C and δ^{18} O) and X-ray microtomography. Pol. Polar Res. 34, 23–38.
- Boy, J.A., Schindler, T., 2000. Ökostratigraphische Bioevents im Grenzbereich
- 686 Stephanium/Autunium (höchstes Karbon) des Saar-Nahe-Beckens (SW-Deutchland)
 687 und benachbarter Gebiete. Neues. Jahrb. Geol. Palaontol. Abh. 216, 89–152.
- Brudefold, F., Soremark, R., 1967. Chapter 18 Chemistry of the mineral phase of enamel. in:
- Miles, A.E.W. (Ed.), Structural and Chemical Organization of Teeth. Academic Press
 Inc, New York, pp. 247–277.
- Bryant, J.D., Froelich, P.N., Showers, W.J., Genna, B.J., 1996. Biologic and climatic signals
 in the oxygen isotopic composition of Eocene-Oligocene equid enamel phosphate.
 Palaeogeogr, Palaeoclimatol, Palaeoecol. 126, 75–8.
- Burrow, C.J., den Blaauwen, J., Newman, M., Davidson, R., 2016. The diplacanthid fishes
- 695 (Acanthodii, Diplacanthiformes, Diplacanthidae) from the Middle Devonian of
 696 Scotland. Palaeontol. Electron. 19, 1–83.
- Burrow, C.J., Davidson, R.G., Den Blaauwen, J.L., Newman, M.J., 2015. Revision of
- 698 Climatius reticulatus Agassiz, 1844 (Acanthodii, Climatiidae), from the Lower
- Devonian of Scotland, based on new histological and morphological data. J. Vertebr.Paleontol. 35, e913421.
- Carey, F. G., Teal, J. M., 1969. Regulation of body temperature by the bluefin tuna. Comp.
 Biochem. Physiol. 28, 205–213.

703	Carpenter, D., Falcon-Lang, H.J., Benton, M.J., Nelson, J.W., 2011. Fishes and tetrapods in
704	the Upper Pennsylvanian (Kasimovian) Cohn coal member of the Mattoon formation
705	of Illinois, United States: systematics, paleoecology, and paleoenvironments. Palaios.
706	26, 619–657.
707	Casanova, J., Hilaire-Marcel, C., 1992. Late Holocene hydrological history of Lake
708	Tanganyika, East Africa, from isotopic data on fossil stromatolites. Palaeogeogr,
709	Palaeoclimatol, Palaeoecol. 91, 35–48.
710	Cerling, T.E., Harris, J.M., 1999. Carbon isotope fractionation between diet and bioapatite in

- 711 ungulate mammals and implications for ecological and paleoecological studies.
 712 Oecologia. 120, 347–363.
- Châteauneuf, J.J., 1980. Synthèse géologique des bassins permiens français. Mém. BRGM.
 82, 1–124.
- Châteauneuf, J.J., Farjanel, G., 1989. Synthèse géologique des bassins permiens français.
 Mém. BRGM. 1–128.
- Châteauneuf, J.J., Farjanel, G., Pacaud, G., Broutin, J., 1992. The Autun permian basin, the
 autunian startotype. Cah. Micropaléontol. 7, 123–139.
- 719 Chen, B., Joachimski, M.M., Shen, S.-Z., Lambert, L.L., Lai, X.L., Wang, X.-D., Chen, J.,
- Yuan, D.X., 2013. Permian ice volume and palaeoclimate history: Oxygen isotope
 proxies revisited. Gondwana Res. 24, 77–89.
- Claypool, G.E., Holser, W.T., Kaplan, I.R., Sakai, H., Zak, I., 1980. The age curves of sulfur
 and oxygen isotopes in marine sulfate and their mutual interpretation. Chem. Geol. 28,
 199–260.
- Clementz, M.T., Koch, K.L., 2001. Differentiating aquatic mammal habitat and foraging
 ecology with stable isotopes in tooth enamel. Oecologia. 129, 461–472.

- Compagno, L.J.V., 1990. Alternative life-history styles of cartilaginous fishes in time and
 space. Environ. Biol. Fishes. 28, 33–75.
- Coplen, T.B., Brand, W.A., Gehre, M., Gröning, M., Meijer, H.A.J., Toman, B., Verkouteren,
 R.M., 2006. New guidelines for ¹³C measurements, Anal. Chem. 78, 2439–2441.
- Crowson, R.A., Showers, W.J., Wright, E.K., Hoering, T.C., 1991. Preparation of Phosphate
 Samples for Oxygen Isotope Analysis. Anal. Chem. 63, 2397–2400.
- Curtis, J.H., Hodell, D.A., Brenner, M., 1996. Climate variability on the Yucatan Peninsula
 (Mexico) during the past 3500 years, and implications for Maya cultural evolution.
 Quat. Res. 46, 37–47.
- 736 Dansgaard, W., 1964. Stable isotopes in precipitation. Tellus. 16, 436–468.
- Davies, S.J., Leng, M.J., Macquaker, J.H.S., Hawkins, K., 2012. Sedimentary process control
 on carbon isotope composition of sedimentary organic matter in an ancient shallowwater shelf succession. Geochem. Geophys. Geosystems. 13, Q0AI04.
- DeAngelis, B.M., McCandless, C.T., Kohler, N.E., Recksiek, C.W., Skomal, G.B., 2008. First
 characterization of shark nursery habitat in the United States Virgin Islands: evidence

of habitat partitioning by two shark species. Mar. Ecol. Prog. 358, 257–271.

- 743 Debriette, P., 1992. Le bassin de Bourbon-l'Archambault et le sillon houillier (Allier, France).
- Présentation et itinéraire géologique. Bulletin Trimestriel de la Société d'Histoire
 Naturelle des Amis du Muséum d'Autun. 144, 13–34.
- 746 Ducassou, C., Bourquin, S., Pellenard, P., Beccaletto, L., Mercuzot, M., Rossignol, C.,
- 747 Poujol, M., Hallot, E., Pierson-Wickmann, A.-C., Gand, G., 2018. Caractérisation
- 748 pétro-géochimique et datation U/Pb du volcanisme contemporain des bassins d'âge
- 749 fini-Carbonifère à Permien du Nord du Massif Central. 26ème Réunion des Sciences
- 750 de la Terre, Lille.

751	Fischer, J., Schneider, J.W., Voigt, S., Joachimski, M.M., Tichomirowa, M., Tütken, T.,
752	Götze, J., Berner, U., 2013. Oxygen and strontium isotopes from fossil shark teeth:
753	Environmental and ecological implications for Late Palaeozoic European basin. Chem.
754	Geol. 342, 44–62.
755	Fischer, J., Schneider, J.W., Hodnett, JP.M., Elliott, D.K., Johnson, G.D., Voigt, S.,
756	Joachimski, M.M., Tichomirowa, M., Götze, J., 2014. Stable and radiogenic isotope
757	analyses on shark teeth from the Early to the Middle Permian (Sakmarian-Roadian) of
758	the southwestern USA. Hist. Biol. 26, 710–727.
759	Fourel F., Martineau F., Seris M., Lécuyer C., 2014. Simultaneous N, C, S stable isotope
760	analyses using new purge and trap technology. Rapid Commun. Mass Spectrom. 28,
761	2587–2594.
762	Fourel F., Martineau F., Seris M., Lécuyer C., 2015. Determination of δ^{34} S of NBS120c and
763	BCR32 phosphorites using purge and trap EA-IRMS technology. Geostand. Geoanal.
764	Res. 39, 47–53.
765	Fourel, F., Martineau, F., Tóth, E.E., Görög, A., Escarguel, G., Lécuyer, C., 2016. Carbon and
766	oxygen isotope variability among foraminifera and ostracod carbonated shells. Ann.
767	UMCS sectio AAA–Physica. 70, 133.
768	Fourel, F., Martineau, F., Lécuyer, C., Kupka, H.J., Lange, L., Ojeimi, C., Seed, M., 2011.
769	¹⁸ O/ ¹⁶ O ratio measurements of inorganic and organic materials by elemental analysis-
770	pyrolysis-isotope ratio mass spectrometry continuous-flow technique. Rapid Com.
771	Mass Spectrom. 25, 2691–2696.
772	Fricke, H.C., Clyde, W.C., O'Neil, J.R., Gingerich, P.D., 1998. Evidence for rapid climate
773	change in North America during the latest Paleocene thermal maximum: oxygen
774	isotope compositions of biogenic phosphate from the Bighorn Basin
775	(Wyoming). Earth Planet. Sci. Lett. 160, 193–208.

776	Friedman, I., O'Neil, J., Cebula, G., 1982. Two new carbonate stable isotope standards.
777	Geostand. newsl. 6, 11–12.
778	Gand, G., Steyer, JS., Chabard, D., 2011. Reprise de fouilles paléontologiques dans un gîte
779	bourgignon célèbre : les "schistes bitumineux" de l'Autunien de Muse (Bassin
780	d'Autun) Bilan 2010 et perspectives. Bourgogne-Franche-Comté Nature. 12, 10-29.
781	Gand, G., Pellenard, P., Galtier, J., Broutin, J., Steyer, JS., 2017. Le stratotype autunien du
782	bassin d'Autun (Bourgogne-France) : évolution de la stratigraphie et des âges. Bulletin
783	Trimestriel de la Société d'Histoire Naturelle des Amis du Muséum d'Autun. 211, 19-
784	36.
785	Gand, G., Steyer, J.S., Pellenard, P., Béthoux, O., Odin, G., Rouchon, V., Van Waveren, I., de
786	Ploeg, G., Chabard, D., 2015. Le stratotype autunien (Permien) du bassin d'Autun:
787	résultats préliminaires des travaux réalisés en 2014 sur les niveaux de la couche de
788	Muse (Saône-et-Loire, France). Bulletin Trimestriel de la Société d'Histoire Naturelle
789	des Amis du Muséum d'Autun. 207, 12–31.
790	Gang, L., Baorong, G., Ermi, Z., 2004. Andrias davidianus. The IUCN Red List of
791	Threatened Species e.T1272A3375181.
792	Ginter, M., Hampe, O., Duffin, C.J., 2010. Handbook of Paleoichthylology - Volume 3D-
793	Chondrichtyes - Paleozoic Elasmobranchii: Teeth, Schultze, HP., Kuhn, O. (Eds.),
794	Verlag Dr. Friedrich Pfeil, Munich, 168 pp.
795	Goedert, J., 2017. Écologie des premiers tétrapodes dévoilée par la composition isotopique du
796	soufre ${}^{(34}S/{}^{32}S)$ de leurs squelettes. Unpublished Ph. D. thesis, Université Claude
797	Bernard Lyon 1, Villeurbanne, 239 pp.
798	Goedert, J., Fourel, F., Amiot, R., Simon, L., Lécuyer, C., 2016. High-precision ³⁴ S/ ³² S
799	measurements in vertebrate bioapatites using purge-and-trap elemental

- analyser/isotope ratio mass spectrometry technology. Rapid Commun. Mass Spectrom.
 30, 2002–2008.
- Goedert, J., Amiot, R., Berthet, D., Fourel, F., Simon, L., Lécuyer, C., 2020. Combined
 oxygen and sulphur isotope analysis—a new tool to unravel vertebrate (paleo)ecology. Sci. Nat. 107, 1–9.
- 805 Goedert, J., Lécuyer, C., Amiot, R., Arnaud-Godet, F., Wang, X., Cui, L., Cuny, G., Douay,
- 806 G., Fourel, F., Panczer, G., Simon, L., Steyer, J.-S., Zhu, M., 2018. Euryhaline
 807 ecology of early tetrapods revealed by stable isotopes. Nature. 558, 68–72.
- Goldman, K. J., 1997. Regulation of body temperature in the white shark, *Carcharodon carcharias*. J. Comp. Physiol. B. 167, 423–429.
- Haesemeyer, M., 2020. Thermoregulation in fish. Mol. Cell. Endocrinol. 518, 110986.
- 811 Halas, S., Szaran, J., 2001. Improved thermal decomposition of sulfates to SO₂ and mass 812 spectrometric determination of δ^{34} S of IAEA SO-5, IAEA SO-6 and NBS-127 sulfate

standards. Rapid Commun. Mass Spectrom. 15, 1618–1620.

Halas, S., Skrzypek, G., Meier-Augenstein, W., Pelc, A., Kemp, H.F., 2011. Inter-laboratory

- 815 calibration of new silver orthophosphate comparison materials for the stable oxygen
- isotope analysis of phosphates. Rapid Commun. Mass Spectrom. 25, 579–584.
- Hampe, O., 2003. Revision of the Xenacanthida (Chondrichthyes: Elasmobranchii) from the
 Carboniferous of the British Isles. Earth Environ. Sci. Trans. R. Soc. Edinb. 93, 191–
 237.
- 820 Hampe, O., Johnson, G.D., Turner, S., 2006. *Dicentrodus* (Chondrichthyes: Xenacanthida)
- from the Early Carboniferous (Visean: upper St Louis Formation) of Iowa, USA.
- 822 Geol. Mag. 143, 545–549.
- Heyler, D., 1969. Vertébrés de l'Autunien de France, Centre National de la Recherche
 Scientifique, Paris, 259 pp.

825	Horton, T.W., Defliese, W.F., Tripati, A.K., Oze, C., 2015. Evaporation induced ¹⁸ O and ¹³ C
826	enrichment in lake systems: A global perspective on hydrologic balance effects. Quat.
827	Sci. Rev. 131, 365–379.
828	Hut, G., 1987. Stable Isotope Reference Samples for Geochemical and Hydrological
829	Investigations, International Atomic Energy Agency, Vienna, 42 pp.
830	Iacumin, P., Bocherens, H., Mariotti, A., Longinelli, A., 1996. Oxygen isotope analyses of co-
831	existing carbonate and phosphate in biogenic apatite: a way to monitor diagenetic
832	alteration of bone phosphate? Earth Planet. Sci. Lett. 142, 1-6.
833	Jerve, A., Bremer, O., Sanchez, S., Ahlberg, P.E., 2017. Morphology and histology of
834	acanthodian fin spines from the late Silurian Ramsåsa E locality, Skåne, Sweden.
835	Palaeontol. Electron. 20.3.56A, 1–19.
836	Joachimski, M.M., von Bitter, P.H., Buggisch, W., 2006. Constraints on Pennsylvanian
837	glacioeustatic sea-level changes using oxygen isotopes of conodont apatite. Geology.
838	34, 277–280.
839	Joachimski, M.M., Van Geldern, R., Breisig, S., Buggisch, W., Day, J., 2004. Oxygen isotope
840	evolution of biogenic calcite and apatite during the Middle and Late Devonian. Int. J.
841	Earth Sci. 93, 542–553.
842	Joachimski, M.M., Breisig, S., Buggisch, W., Talent, J.A., Mawson, R., Gereke, M., Morrow,
843	J.R., Day, J., Weddige, K., 2009. Devonian climate and reef evolution: insights from
844	oxygen isotopes in apatite. Earth Planet. Sci. Lett. 284, 599-609.
845	Johnson, G.D., 1999. Dentitions of Late Palaeozoic Orthacanthus species and new species
846	of ?Xenacanthus (Chondrichthyes: Xenacanthiformes) from North America. Acta
847	Geol. Pol. 49, 215–266.
848	Kaplan, I.R., 1983. Stable isotopes of sulfur, nitrogen and deuterium in recent marine
849	environments, in: Arthur, M.A., Anderson, T.F., Kaplan, I.R., Veizer, J., Land, L.S.,

- 850 (Eds.), Stable Isotopes in Sedimentary Geology. Society of Economic Paleontologists
 851 and Mineralogists Short Course, Dallas, pp. 2.1–2.108.
- 852 Katsev, S., Crowe, S.A., Mucci, A., Sundby, B., Nomosatryo, S., Haffner, D.G., Fowlef,
- D.A., 2010. Mixing and its effects on biogeochemistry in the persistently stratified,
 deep, tropical Lake Matano, Indonesia. Limnol. Oceanogr. 55, 763–776.
- 855 Kaulfuß, U., 2003. Lithofazies, Genese und Stratigraphie des Permokarbon im Becken von
- 856 Bourbon-l`Archambault (Massif central) Fallstudie Buxières-les-Mines.
- 857 Unpublished Master thesis, Bergakademie Freiberg Technische Universität, Freiberg,
 858 82 pp.
- Koch, P.L., Tuross, N., Fogel, M.L., 1997. The Effects of Sample Treatment and Diagenesis
 on the Isotopic Integrity of Carbonate in Biogenic Hydroxylapatite. J. Archaeol. Sci.
 24, 417–429.
- Kolodny, Y., Luz, B., 1991. The isotopic record of oxygen in phosphates of fossil fish-
- B63 Devonian to Recent, in: Taylor, H.P. Jr., O'Neil, R., Kaplan, I.R. (Eds.), Stable isotope
- 864 geochemistry: A tribute to Samuel Epstein. The Geochemical Society, Special
- 865 Publication, Alexandria, pp. 105–119.
- Kolodny, Y., Luz, B., Navon, O., 1983. Oxygen isotope variations in phosphate of biogenic
 apatites, I. Fish bone apatite—rechecking the rules of the game. Earth Planet. Sci. Lett.
 64, 398–404.
- Kriwet, J., Witzmann, F., Klug, S., Heidtke, U.H.J., 2008. First direct evidence of a vertebrate
 three-level trophic chain in the fossil record. Proc. Royal Soc. B. 275, 181–186.
- 871 Krouse, H.R. 1980. Sulphur isotopes in our environment, in: Fritz, P., Fontes, J.C. (Eds.),
- Isotope Geochemistry, Vol. 1. The Terrestrial Environment. Elsevier, Amsterdam, pp.
 435–71.

874	Kutzbach, J.E., Ziegler, A.M., 1994. Simulation of Late Permian climate and biomes with an
875	atmosphere-ocean model: comparisons with observations. Philos. Trans. R. Soc.
876	Lond., B, Biol. Sci. 341, 327–340.

- Laurin, M., Soler-Gijón, R., 2010. Osmotic tolerance and habitat of early stegocephalians:
 indirect evidence from parsimony, taphonomy, palaeobiogeography, physiology and
 morphology. Geol. Soc. Spec. Publ. 339, 151–179.
- Lécuyer, C., Amiot, R., Touzeau, A., Trotter, J., 2013. Calibration of the phosphate δ¹⁸O
 thermometer with carbonate–water oxygen isotope fractionation equations. Chem.
 Geol. 347, 217–226.
- Lécuyer, C., Grandjean, P., O'Neil, J.R., Cappetta, H., Martineau, F., 1993. Thermal
 excursions in the ocean at the Cretaceous-Tertiary boundary (northern Morocco): δ¹⁸O
- record of phosphatic fish debris. Palaeogeogr, Palaeoclimatol, Palaeoecol. 105, 235–
 243.
- Lécuyer, C., Bogey, C., Garcia, J.P., Grandjean, P., Barrat, J.A., Floquet, M., Bardet, N.,
- 888 Pereda-Superbiola, X., 2003. Stable isotope composition and rare earth element
- content of vertebrate remains from the Late Cretaceous of northern Spain (Laño): did
- the environmental record survive? Palaeogeogr, Palaeoclimatol, Palaeoecol. 193, 457–
- 891 471.
- Lewis Jr, W.M., 1987. Tropical limnology. Annu. Rev. Ecol. Syst. 18, 159–184.
- 893 Li, H.C., Ku, T.L., 1997. δ^{13} C $-\delta^{18}$ C covariance as a paleohydrological indicator for closed-894 basin lakes. Palaeogeogr, Palaeoclimatol, Palaeoecol. 133, 69–80.
- 895 Luccisano, V., Pradel, A., Amiot, R., Gand, G., Steyer, J. S., & Cuny, G., 2021. A new
- 896 *Triodus* shark species (Xenacanthidae, Xenacanthiformes) from the lowermost
- 897 Permian of France and its paleobiogeographic implications. J Vertebr Paleontol. 41,
- 898 e1926470.

899	Luccisano, V., Pradel, A., Amiot, R., Pouillon, J. M., Kindlimann, R., Steyer, JS., Cuny, G.,
900	2022. Systematics, ontogeny and palaeobiogeography of the genus Orthacanthus
901	(Diplodoselachidae, Xenacanthiformes) from the lower Permian of France. Pap.
902	Palaeontol. 8, e1470.
903	Maisey, J.G., 1978. Growth and Form of finspines in Hybodont sharks. Palaeontology. 21,
904	657–666.
905	Maisey, J.G., 1979. Finspine morphogenesis in squalid and heterodontid sharks. Zool. J. Linn.
906	Soc. 66, 161–183.
907	Maisey, J.G., 1982. Studies on the Paleozoic selachian genus Ctenacanthus Agassiz. No. 2,
908	Bythiacanthus St. John and Worthen, Amelacanthus, new genus, Eunemacanthus St.
909	John and Worthen, Sphenacanthus Agassiz, and Wodnika Münster. Am. Mus. Novit.
910	2722, 1–24.
911	Marteau, P., 1983. Le bassin permo carbonifère d'Autun: stratigraphie, sédimentologie et
912	aspects structuraux. Unpublished Ph.D. Thesis, Université de Dijon, Dijon, 183 pp.
913	McConnaughey, T. A., Burdett, J., Whelan, J. F., & Paull, C. K., 1997. Carbon isotopes in
914	biological carbonates: respiration and photosynthesis. Geochim. Cosmochim.
915	Acta. 61, 611–622.
916	Mercuzot, M., 2020. Reconstitutions paléoenvironnementales et paléoclimatiques en contexte
917	tardi-orogénique : cas des bassins fini carbonifères à permiens du nord-est du Massif
918	central, France. Unpublished Ph.D. Thesis, Université de Rennes 1, Rennes, 551 pp.
919	Mercuzot, M., Bourquin, S., Pellenard, P., Beccaletto, L., Schnyder, J., Baudin, F., Ducassou,
920	C., Garel, S., Gand, G., 2022. Reconsidering Carboniferous-Permian continental
921	paleoenvironments in eastern equatorial Pangea: facies and sequence stratigraphy
922	investigations in the Autun Basin (France). Int. J. Earth Sci. 111, 1663–1696.

- 923 Nehlich, O., 2015. The application of sulphur isotope analyses in archaeological research: a
 924 review. Earth Sci. Rev. 142, 1–17.
- 925 Olson, E.C., 1989. The Arroyo Formation (Leonardian, Lower Permian) and its vertebrate
 926 fossils. T. Mem. Mus. Bull. 33, 1–25.
- 927 Otero, O., Lécuyer, C., Fourel, F., Martineau, F., Mackaye, H.T., Vignaud, P., Brunet, M.,
- 928 2010. Freshwater fish δ¹⁸O indicates a Messinian change of the precipitation regime in
 929 Central Africa. Geology. 39, 435–438.
- 930 Pandian, T.J., Vivekanandan, E., 1985. Energetics of Feeding and Digestion, in: Tytler, P.,
- 931 Calow, P. (Eds.), Fish Energetics. Springer, Dordrecht, pp. 99–124.
- Paquette, Y., Doubinger, J., Courel, L., 1980. Étude palynologique de la couche du toit du
- 933 bassin autunien de l'Aumance (assise de Buxières): liaison avec les milieux
- 934 sédimentaires. Bulletin Trimestriel de la Société d'Histoire Naturelle des Amis du
 935 Muséum d'Autun. 95, 85–101.
- Parrish, J.T., 1993. Climate of the supercontinent Pangea. J. Geol. 101, 215–233.
- 937 Passey, B. H., Robinson, T. F., Ayliffe, L. K., Cerling, T. E., Sponheimer, M., Dearing, M.
- D., Roeder, B. L., Ehleringer, J. R., 2005. Carbon isotope fractionation between diet,
 breath CO₂, and bioapatite in different mammals. J. Archaeol. Sci. 32. 1459–1470.
- 940 Passey, B.H., Cerling, T.E., Levin, N.E., 2007. Temperature dependence of oxygen isotope
- acid fractionation for modern and fossil tooth enamels. Rapid Commun. MassSpectrom. 21, 2853–2859.
- 943 Paytan, A., Yao, W., Faul, K.L., Gray, E.T., 2020. Application of sulphur isotopes for
- 944 stratigraphic correlation, in: Gradstein, F. M., Ogg, J.G., Schmitz, M.D., Ogg, G.M.
- 945 (Eds.), Geologic Time Scale 2020, Elsevier, Amsterdam, pp. 259–278.

946	Pellenard, P., Gand, G., Schmitz, M., Galtier, J., Broutin, J., Steyer, JS., 2017. High-
947	precision U-Pb zircon ages for explosive volcanism calibrating the NW European
948	continental Autunian stratotype. Gondwana Res. 51, 118-136.
949	Pruvost, P., 1942. Étude géologique du bassin Permo-Carbonifère d'Autun, BRGM, Orléans-
950	la-Source. 23 pp.
951	Rees, C.E., Jenkins, W.J., Monster, J. 1978. The sulphur isotopic composition of ocean water

0017 II. 1

sulphate. Geochim. Cosmochim. Acta. 42, 377–381.

- 953 Reif, W.-E., 1978. Types of morphogenesis of the dermal skeleton in fossil sharks. PalZ. 52,
 954 110–128.
- Rink, W.J., Schwarcz, H.P., 1995. Tests for diagenesis in tooth enamel: ESR dating signals
 and carbonate contents. J. Archaeol. Sci. 22, 251–255.
- 857 Roscher, M., Schneider, J.W., 2006. Permo-Carboniferous climate: Early Pennsylvanian to
 858 Late Permian climate development of central Europe in a regional and global context.
- 959 Geol. Soc. Spec. Publ. 265, 95–136.
- Salzburger, W., Van Bocxlaer, B., Cohen, A.S., 2014. Ecology and evolution of the African
 Great Lakes and their faunas. Annu. Rev. Ecol. Evol. Syst. 45, 519–545.
- 962 Santos, G. M., Ferguson, J., Acaylar, K., Johnson, K. R., Griffin, S., & Druffel, E., 2011.
- 963 Δ^{14} C and δ^{13} C of seawater DIC as tracers of coastal upwelling: A 5-year time series 964 from Southern California. Radiocarbon. 53, 669–677.
- Schneider, J.W., 1996. Xenacanth teeth a key for taxonomy and biostratigraphy. Mod. Geol.
 20, 321–340.
- Schneider, J.W., Werneburg, R., 2006. Insect biostratigraphy of the Euramerican continental
 late Pennsylvanian and early Permian. Geol. Soc. Spec. Publ. 265, 325–336.

969	Schneider, J.W., Hampe, O., Soler-Gijón, R., 2000. The Late Carboniferous and Permian:
970	Aquatic vertebrate zonation in southern Spain and German basins. Cour. Forsch. Inst.
971	Senckenberg. 223, 543–561.
972	Schultze, HP., 1985. Marine to onshore vertebrates in the Lower Permian of Kansas and
973	their paleoenvironmental implications. Univ. Kans. Paleontol. Contrib. 113, 1–18.
974	Schultze, HP., 1995. Terrestrial biota in coastal marine deposits: Fossil-lagerstätten in the
975	Pennsylvanian of Kansas, USA. Palaeogeogr, Palaeoclimatol, Palaeoecol. 119, 255-
976	273.
977	Schultze, HP., 1998. The Fossil Record of the Intertidal Zone, in: Horn, M.H., Martin,
978	K.L.M., Chotkowski, M.A. (Eds.), Intertidal Fishes. Life in Two Worlds. Academic
979	Press, San Diego, pp. 373–392.
980	Schultze, HP., 2009. Interpretation of marine and freshwater paleoenvironments in Permo-
981	Carboniferous deposits. Palaeogeogr, Palaeoclimatol, Palaeoecol. 281, 126–136.
982	Schultze, HP., 2013. The palaeoenvironments at the transition from piscine to tetrapod
983	sarcopterygians. Bull. N. M. Mus. Nat. Hist. Sci. 60, 373-397.
984	Schultze, HP., Soler-Gijón, R., 2004. A xenacanth clasper from the ?uppermost
985	Carboniferous - Lower Permian of Buxières-les-Mines (Massif Central, France) and
986	the palaeoecology of the European Permo-Carboniferous basins. Neues. Jahrb. Geol.
987	Palaontol. Abh. 232, 325–363.
988	Shackleton, N.J., 1975. Paleotemperature history of the Cenozoic and the initiation of
989	Antarctic glaciation: oxygen and carbon isotope analyses in DSDP sites 277, 279 and
990	281. Init. Repts. DSDP. 29, 743-755.
991	Soler-Gijón, R., 1993. The xenacanth sharks from the Upper Stephanian of the Puertollano
992	basin (Spain). J. Vertebr. Paleontol. 13, 58A.

- Soler-Gijón, R., 1995. Evidence of predator-prey relationship in xenacanth sharks of the
- 994 Upper Carboniferous (Stephanian C) from Puertollano, Spain. Geobios. 28, 151–156.
- 995 Soler-Gijón, R., 1999. Occipital Spine of *Orthacanthus* (Xenacanthidae, Elasmobranchii):
- Structure and Growth. J. Morphol. 242, 1–45.
- Soler-Gijón, R., Moratalla, J.J., 2001. Fish and tetrapod trace fossils from the Upper
 Carboniferous of Puertollano, Spain. Palaeogeogr, Palaeoclimatol, Palaeoecol. 171, 1–
 28.
- Štamberg, S., Schneider, J.W., Werneburg, R., 2016. Fossil fauna and flora of a re-discovered
 locality in the Late Carboniferous Ploužnice Horizon of the Krkonoše Piedmont Basin,
 Bohemian Massif. Foss. Imp. 72, 215–224.
- 1003 Steyer, J.-S., Escuillié, F., Pouillon, J.-M., Broutin, J., Debriette, P., Freytet, P., Gand, G.,
- 1004 Poplin, C., Rage, J.-C., Rival, J., Schneider, J.W., Štamberg, S., Werneburg, R., Cuny,
- 1005 G., 2000. New data on the flora and fauna from the ?uppermost Carboniferous-Lower
- 1006 Permian of Buxières-les-Mines, Bourbon l'Archambault Basin (Allier, France).
- 1007 preliminary report. Bull. Soc. Géol. Fr. 171, 239–249.
- 1008 Stichler, W., 1995. Interlaboratory comparison of new materials for carbon and oxygen
- isotope ratio measurements. Reference and intercomparison materials for stable
 isotopes of light elements. 825, 67–74.
- 1011 Thorrold, S. R., Campana, S. E., Jones, C. M., & Swart, P. K., 1997. Factors determining δ^{13} C
- 1012 and δ^{18} O fractionation in aragonitic otoliths of marine fish. Geochim. Cosmochim.
- 1013 Acta. 61, 2909–2919.
- 1014 Trotter, J.A., Williams, I.S., Barnes, C.R., Lécuyer, C., Nicoll, R.S., 2008. Did cooling oceans
- 1015trigger Ordovician biodiversification? Evidence from conodont
- 1016 thermometry. Science. 321, 550–554.

1017	Vennemann, T.W., Hegner, E., Cliff, G., Benz, G.W., 2001. Isotopic composition of recent
1018	shark teeth as a proxy for environmental conditions. Geochim. Cosmochim. Acta. 65,
1019	1583–1599.
1020	Wenzel, B., Lécuyer, C., Joachimski, M.M., 2008. Comparing oxygen isotope records of
1021	Silurian calcite and phosphate— δ^{18} O compositions of brachiopods and conodonts.
1022	Geochim. Cosmochim. Acta. 64, 1859–1872.
1023	Zangerl, R., 1981. Handbook of Paleoichthyology - Chondrichthyes I - Paleozoic
1024	Elasmobranchii, Schultze, HP., Kuhn, O. (Eds.), Gustav Fischer Verlag, Stuttgart,
1025	115 pp.
1026	Zancolli, G., Steffan-Dewenter, I., Rödel, M.O., 2014. Amphibian diversity on the roof of
1027	Africa: unveiling the effects of habitat degradation, altitude and biogeography. Divers.
1028	Distrib. 20, 297–308.
1029	Zazzo, A., Lécuyer, C., Sheppard, S.M., Grandjean, P., Mariotti, A., 2004. Diagenesis and the
1030	reconstruction of paleoenvironments: a method to restore original δ^{18} O values of
1031	carbonate and phosphate from fossil tooth enamel. Geochim. Cosmochim. Acta. 68,
1032	2245–2258.
1033	
1034	Table caption
1035	Table 1. Mean oxygen, carbon and sulfur isotope compositions of the studied vertebrate
1036	bioapatites from Buxières-les-Mines and the Muse OSB. The values are those of each
1037	specimen. For the single sample specimens (n=1), the standard deviation (sd) equals to the
1038	analytical sd of the sample. Abbreviations: n, number of samples. sd, standard deviation.
1039	
1040	Figure captions

42

Figure 1. Geological context. A, simplified geological map showing the location of the Autun 1041 1042 and Bourbon l'Archambault basins in the Northern Massif Central. B, simplified geological map of the Autun Basin. C, simplified geological map of the Bourbon l'Archambault Basin. 1043 **D**, simplified stratigraphy of the Muse OSB. **E**, simplified stratigraphy of Buxière-les-Mines. 1044 The drawings indicate the known or approximative location of investigated specimens and 1045 taxa. Red stars represent the investigated localities of Buxières-les-Mines and Muse OSB. 1046 1047 Abbreviations: LB, Lien Blanc; LV, Lien Vert (modified from Châteauneuf, 1980; Marteau, 1983; Châteauneuf & Farjanel, 1989; Châteauneuf et al., 1992; Stever et al., 2000; Gand et 1048 1049 al., 2011, 2015, 2017; Pellenard et al., 2017). [color]

1050

Figure 2. Growth pattern of xenacanth dorsal spine and sampling strategy on cf. *Orthacanthus*sp. (top) and cf. *Triodus* sp. (bottom). The numbers 1 to 12 are the successive analysed samples
from the apex to the base. Dorsal spine drawings are modified from Beck et al. (2016) for cf. *Orthacanthus* sp. and from Hampe (2003) for cf. *Triodus* sp.

1055

Figure 3. Evolution of the δ¹⁸O_{PO4} values along the xenacanth dorsal spines. A, cf. *Triodus* sp.
individuals from Muse OSB. B, cf. *Orthacanthus* sp. individuals from Buxières-les-Mines. C,
cf. *Triodus* sp. specimens from Buxières-les-Mines. [color]

1059

Figure 4. Evolution of the $\delta^{13}C_{CO3}$ values along the fin spines of three acanthodian (**A**) and the dorsal spine of two xenacanth (**B**) individuals from Buxières-les-Mines and the Muse OSB. [color]

1063

Figure 5. Evolution of the δ^{34} S values along the fin spines of two acanthodian and the dorsal spine of two xenacanth individuals from Buxières-les-Mines and the Muse OSB. [color]

1066

1067 **Figure 6.** Evolution of the $\delta^{18}O_{PO4}$ values along seven acanthodian fin spines from Buxières-1068 les-Mines and the Muse OSB. [color]

1069

- 1070 **Figure 7.** Oxygen isotope composition of bioapatite phosphate ($\delta^{18}O_{PO4}$) from studied
- 1071 vertebrate taxa plotted against their corresponding oxygen isotope composition of bioapatite
- 1072 carbonate ($\delta^{18}O_{CO3}$). The values are plotted with those (in grey and pink) of modern (Iacumin
- et., 1996; Vennemann et al., 2001) and fossil (Kolodny and Luz, 1983; Fricke et al., 1998;
- Lécuyer et al., 2003; Amiot et al., 2010; Goedert et al., 2018) samples from different aquatic
- 1075 environments. The dashed line has a slope of a=1 in order to highlight the correlation between
- 1076 the $d^{18}O_{PO}$ and $d^{18}O_{CO3}$ values. [color]

1077

- **Figure 8.** Difference between the oxygen isotope compositions of bioapatite carbonate
- 1079 ($\delta^{18}O_{CO3}$) and phosphate ($\delta^{18}O_{PO4}$) plotted against the carbonate concentration (CO₃ weight%)
- 1080 of the studied vertebrate taxa. [color]

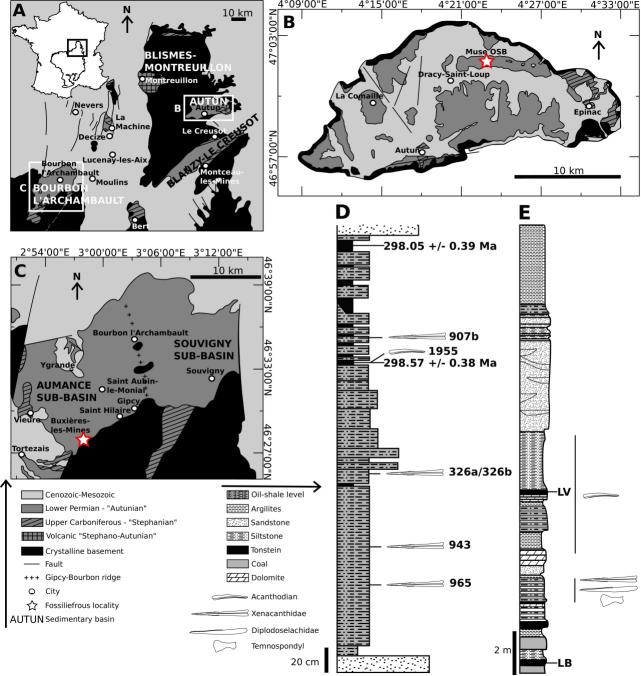
1081

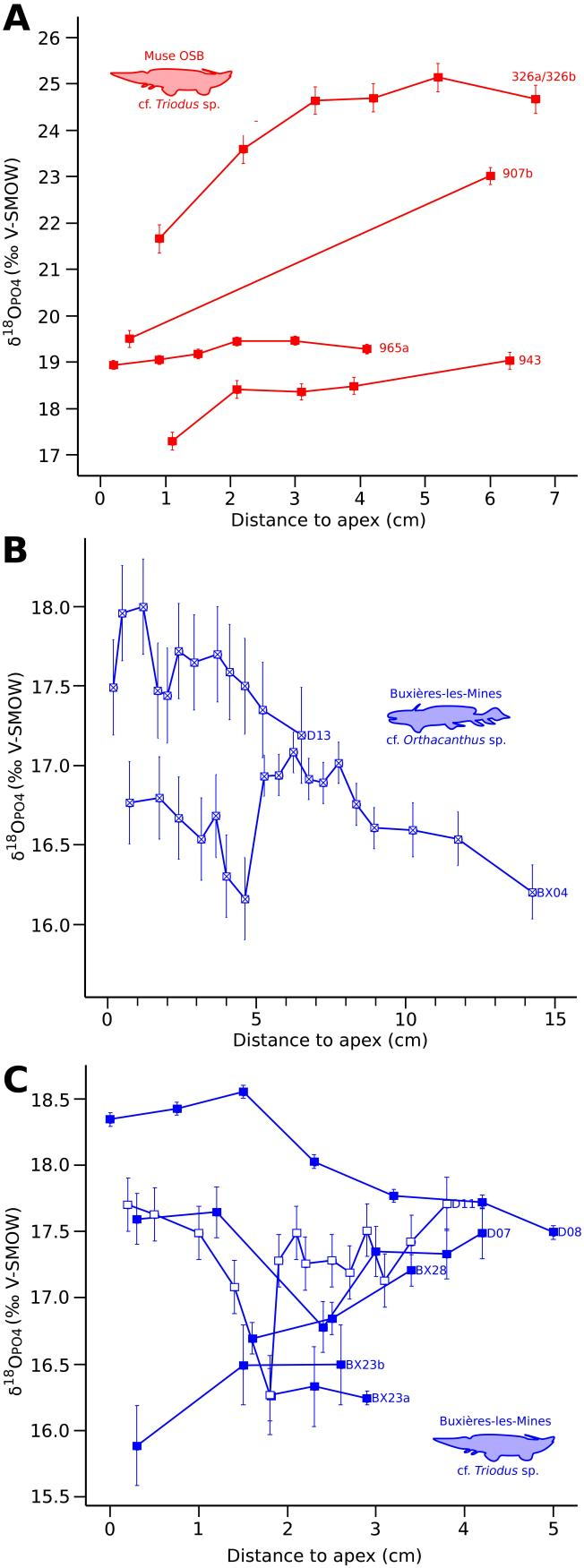
- 1082 **Figure 9.** The sulfur isotope composition of bioapatite (δ^{34} S) plotted against the sulfur content 1083 (weight% S) of the studied vertebrate taxa. [color]
- 1084

Figure 10. Reconstructed palaeotemperature based on the actinopterygians, acanthodians and sharks from Buxières-les-Mines and the Muse OSB. Reconstructed palaeotemperatures using δ^{18} O of modern marine waters are in the left and those using δ^{18} O of modern lake waters are in the right. For each taxonomic group, the dot point is the mean value, and the bars represent the standard deviation. Values used can be seen in Table S2. [color]

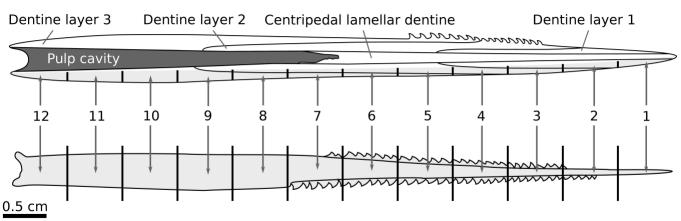
1090

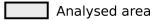
- 1091 Figure 11. Orthacanthus tooth stuck in a temnospondyl dentary in Buxières-les-Mines. A,
- 1092 photograph. **B**, interpretation drawing. [color]
- 1093
- 1094 Figure 12. Environmental reconstructions of the Buxières-les-Mines and Muse OSB
- 1095 localities. The presence of the non-investigated cf. *Lissodus* sp. in Buxières-les-Mines follows
- the faunal list of Steyer et al. (2000). [color]

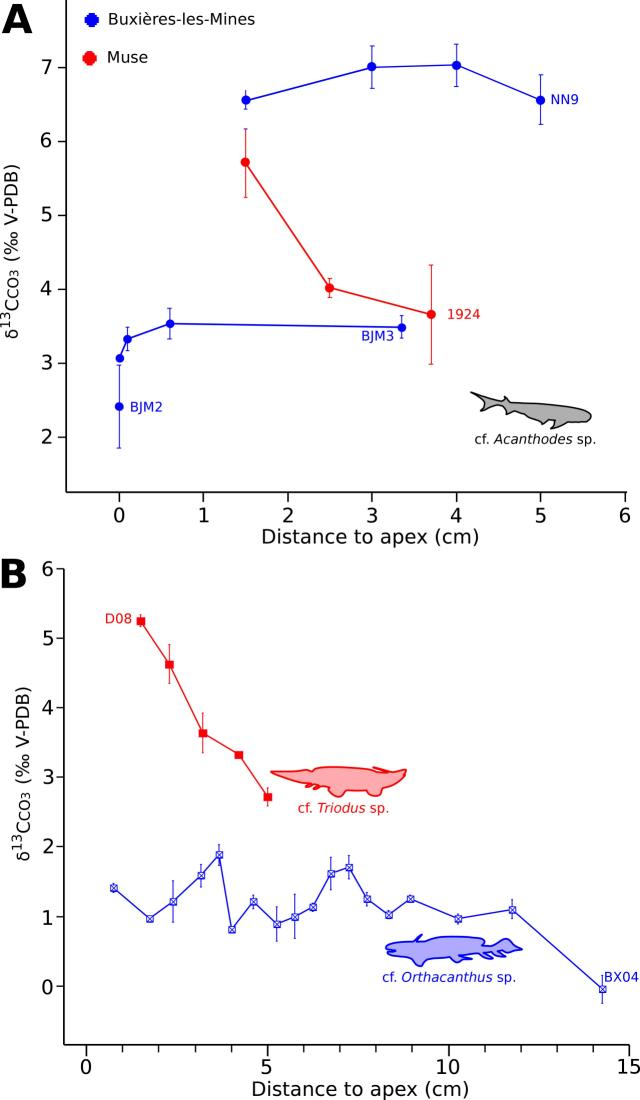


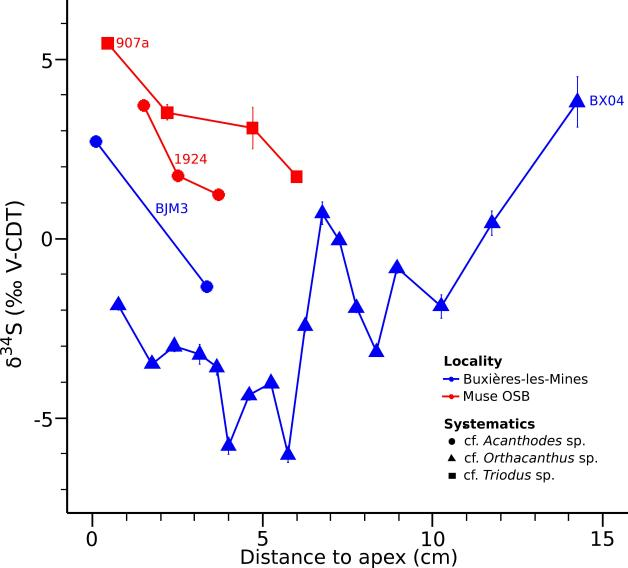


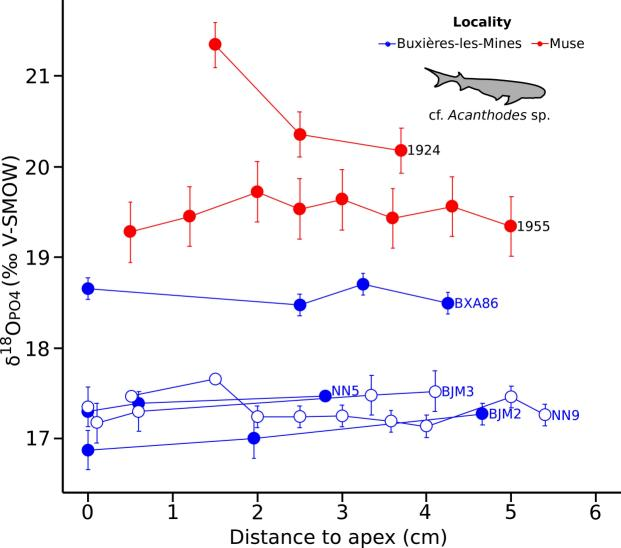
1 cm



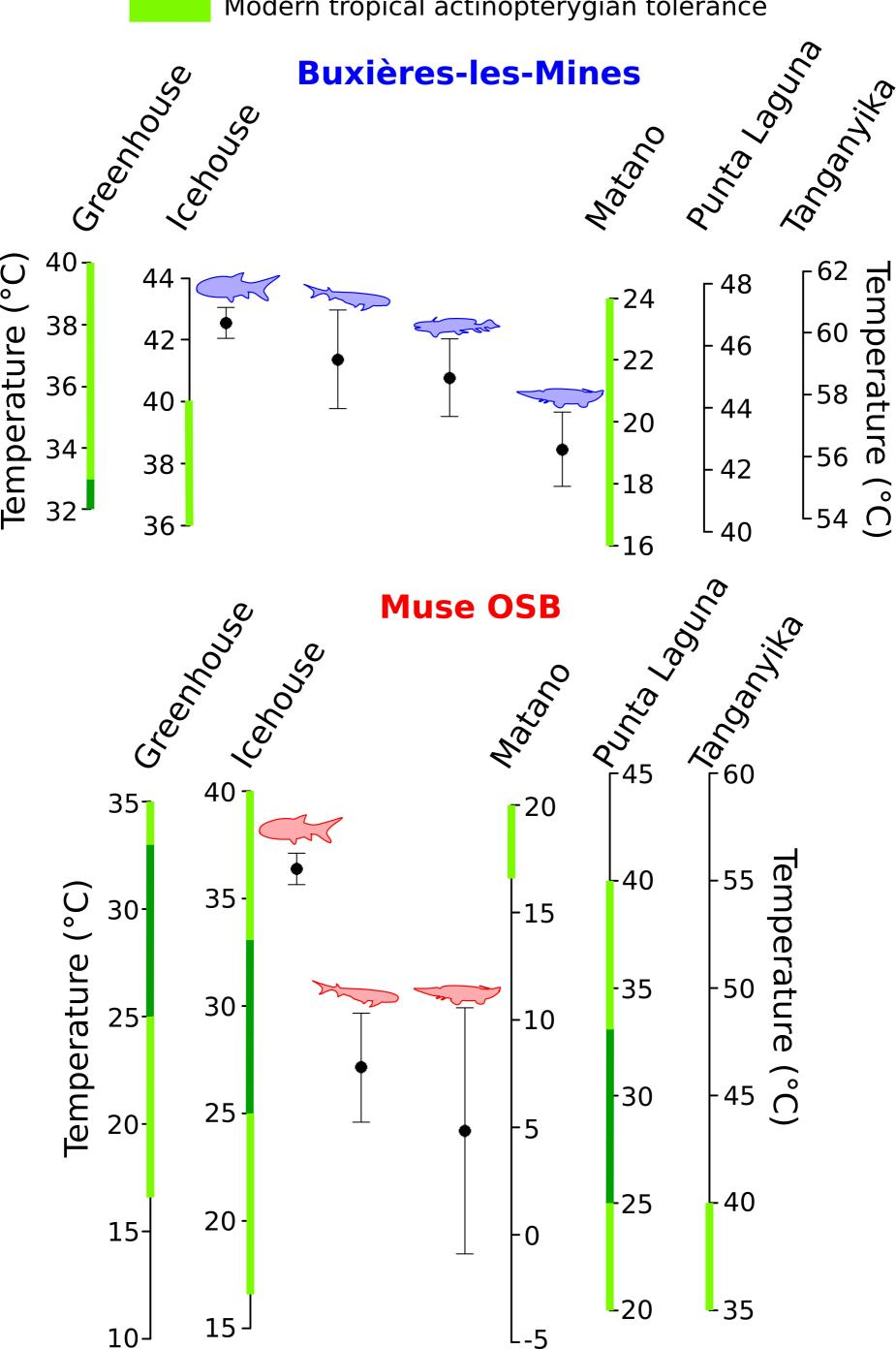


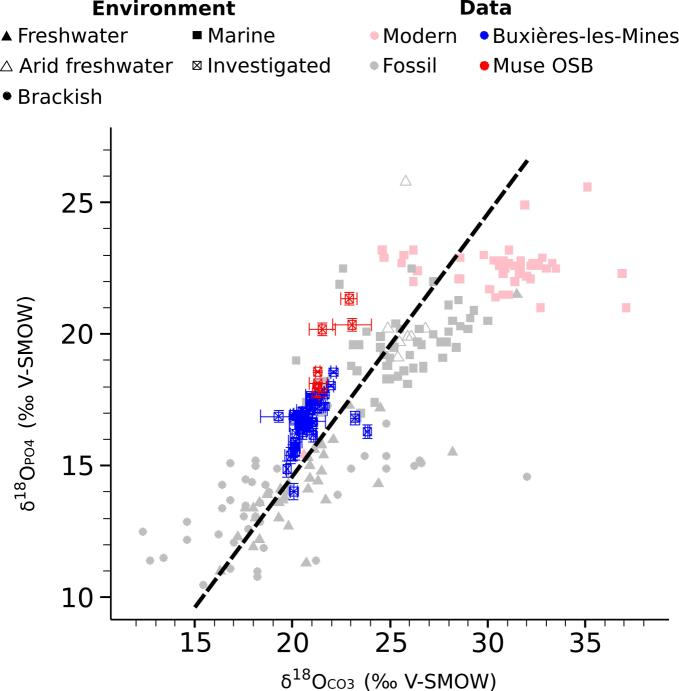


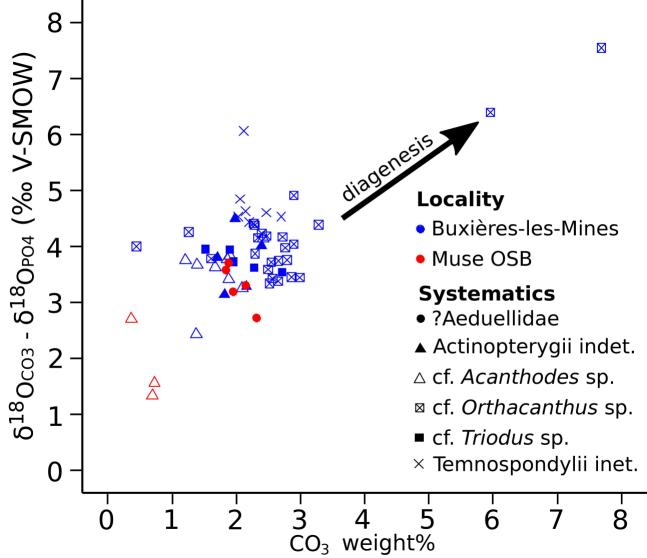


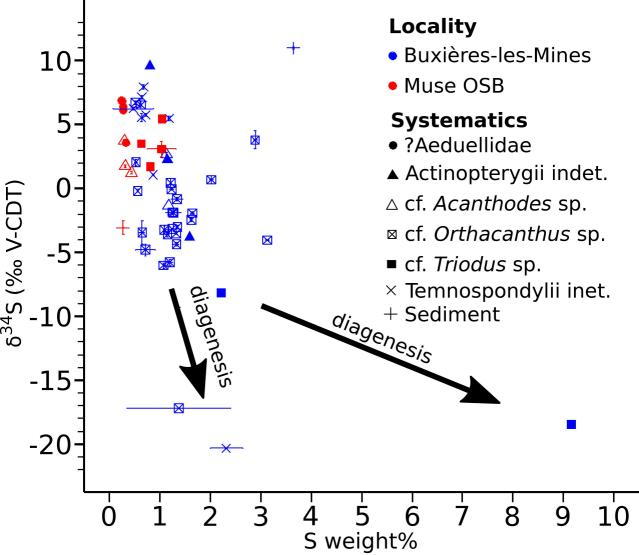


Modern freshwater stingrays tolerance Modern tropical actinopterygian tolerance











B 1 cm

Temnospondyl dentary

